

# Inverse analysis of the structure and dynamics of the whole Newfoundland–Labrador Shelf ecosystem

Claude Savenkoff<sup>1</sup>, Alain F. Vézina<sup>2</sup>, and Alida Bundy<sup>2</sup>

<sup>1</sup> Regional Science Branch,  
Department of Fisheries and Oceans,  
Maurice Lamontagne Institute,  
Mont-Joli (Quebec), Canada G5H 3Z4

<sup>2</sup> Regional Science Branch,  
Department of Fisheries and Oceans,  
Bedford Institute of Oceanography,  
Dartmouth, (Nova Scotia), Canada B2Y 4A2

2001

Canadian Technical Report of  
Fisheries and Aquatic Sciences 2354

## **Canadian Technical Report of Fisheries and Aquatic Sciences**

Technical reports contain scientific and technical information that contribute to existing knowledge but that are not normally appropriate for primary literature. Technical reports are directed primarily toward a worldwide audience and have an international distribution. No restriction is placed on subject matter, and the series reflects the broad interests and policies of the Department of Fisheries and Oceans, namely, fisheries and aquatic sciences.

Technical reports may be cited as full publications. The correct citation appears above the abstract of each report. Each report is indexed in the data base *Aquatic Sciences and Fisheries Abstracts*.

Numbers 1-456 in this series were issued as Technical Reports of the Fisheries Research Board of Canada. Numbers 457-714 were issued as Department of the Environment, Fisheries and Marine Service, Research and Development Directorate Technical Reports. Numbers 715-924 were issued as Department of Fisheries and the Environment, Fisheries and Marine Service Technical Reports. The current series name was changed with report number 925.

Technical reports are produced regionally but are numbered nationally. Requests for individual reports will be filled by the issuing establishment listed on the front cover and title page. Out-of-stock reports will be supplied for a fee by commercial agents.

## **Rapport technique canadien des sciences halieutiques et aquatiques**

Les rapports techniques contiennent des renseignements scientifiques et techniques qui constituent une contribution aux connaissances actuelles, mais qui ne sont pas normalement appropriés pour la publication dans un journal scientifique. Les rapports techniques sont destinés essentiellement à un public international et ils sont distribués à cet échelon. Il n'y a aucune restriction quant au sujet; de fait, la série reflète la vaste gamme des intérêts et des politiques du ministère des Pêches et des Océans, c'est-à-dire les sciences halieutiques et aquatiques.

Les rapports techniques peuvent être cités comme des publications intégrales. Le titre exact paraît au-dessus du résumé de chaque rapport. Les rapports techniques sont indexés dans la base de données *Aquatic Sciences and Fisheries Abstracts*.

Les numéros 1 à 456 de cette série ont été publiés à titre de rapports techniques de l'Office des recherches sur les pêcheries du Canada. Les numéros 457 à 714 sont parus à titre de rapports techniques de la Direction générale de la recherche et du développement, Service des pêches et de la mer, ministère de l'Environnement. Les numéros 715 à 924 ont été publiés à titre de rapports techniques du Service des pêches et de la mer, ministère des Pêches et de l'Environnement. Le nom actuel de la série a été établi lors de la parution du numéro 925.

Les rapports techniques sont produits à l'échelon régional, mais numérotés à l'échelon national. Les demandes de rapports seront satisfaites par l'établissement d'origine dont le nom figure sur la couverture et la page du titre. Les rapports épuisés seront fournis contre rétribution par des agents commerciaux.

Canadian Technical Report of  
Fisheries and Aquatic Sciences 2354

2001

INVERSE ANALYSIS OF THE STRUCTURE AND DYNAMICS  
OF THE WHOLE NEWFOUNDLAND–LABRADOR SHELF ECOSYSTEM

by

Claude Savenkoff<sup>1</sup>, Alain F. Vézina<sup>2</sup>, and Alida Bundy<sup>2</sup>

<sup>1</sup>: Regional Science Branch, Department of Fisheries and Oceans, Maurice Lamontagne Institute,  
P.O. Box 1000, Mont-Joli (Quebec), G5H 3Z4

<sup>2</sup>: Department of Fisheries and Oceans, Bedford Institute of Oceanography, Division of Coastal  
Ocean Science, Dartmouth, Nova Scotia, B2Y 4A2

---

© Minister of Public Works and Government Services Canada 2001  
Cat. No. Fs 97-6/2354E ISSN 0706-6457

Correct citation for this publication:

Savenkoff, C., A.F. Vézina, and A. Bundy. 2001. Inverse analysis of the structure and dynamics of the whole Newfoundland–Labrador Shelf ecosystem. Can. Tech. Rep. Fish. Aquat. Sci. 2354: viii+56 p.

## TABLE OF CONTENTS

	page
LIST OF TABLES .....	iv
LIST OF FIGURES .....	v
LIST OF APPENDICES .....	vi
ABSTRACT/RÉSUMÉ .....	vii
PREFACE .....	viii
INTRODUCTION .....	1
MATERIALS AND METHODS .....	2
DATA USED IN MODELLING .....	2
MODEL STRUCTURE .....	2
MODEL CONSTRAINTS .....	3
MODEL SOLUTION .....	4
NOISE IN THE DATA: SENSITIVITY STUDIES .....	5
RESULTS .....	5
SENSITIVITY OF INVERSE SOLUTIONS .....	5
COMPARISONS OF INVERSE SOLUTIONS .....	6
COMPARISONS WITH THE MASS BALANCE MODEL USING THE ECOPATH APPROACH .....	7
Comparisons of model solutions .....	7
Comparisons of ecotrophic efficiency .....	8
Comparisons of mortality processes .....	8
Comparisons of predation mortality .....	9
Comparisons between specific assumptions to balance the Ecopath model and inverse solution .....	10
<i>Impact of skates</i> .....	11
<i>Large crustacea–small demersal feeders–shrimp trophic triangle</i> .....	11
DISCUSSION .....	12
VALIDITY OF MASS-BALANCE SOLUTIONS .....	12
PREDATION AND TRANSFER EFFICIENCY IN THE NEWFOUNDLAND– LABRADOR SHELF FOR THE 1985-1987 PERIOD .....	14
CONCLUSION .....	15
ACKNOWLEDGEMENTS .....	16
REFERENCES .....	16

## LIST OF TABLES

Table 1.	Functional groups used in inverse modelling for the 1985-1987 period in the Newfoundland–Labrador Shelf .....	18
Table 2.	Input parameters for inverse modelling estimated from Bundy <i>et al.</i> (2000) .....	20
Table 3.	Unknown flows and corresponding weights used in the inverse modelling.....	22
Table 4.	Mass balance and additional equations and corresponding weights used in the inverse modelling.....	23
Table 5.	Constraints on food web processes used in the inverse modelling .....	24
Table 6.	Sums of squared normalized residuals for the compartmental mass balances .....	26
Table 7.	Number of mean flow estimates that are described as small variability (mean > SD) or large variability (mean < SD), and details of large variability terms .....	26
Table 8.	Root mean square difference (RMSD) obtained between the minimum and maximum constraints, between the A1 and A2 models, and between the inverse A2 and Ecopath models on each flow/efficiency .....	27
Table 9.	Consumption and ecotrophic efficiency estimated from inverse and Ecopath modelling.....	28
Table 10.	Diet composition for skates and large crustaceans estimated by inverse modelling.....	30
Table 11.	Mortality rates and details of mortality estimated from the inverse A2 and Ecopath models .....	31
Table 12.	Distribution of predation mortality (PM expressed by prey biomass, $\Sigma Pr_X \rightarrow Y/B_X$ , per year) among vertebrate predators on all prey as estimated from the inverse A2 and Ecopath models .....	32
Table 13.	Comparisons between key global indices of ecosystem structure for the two mass balance models developed for the Newfoundland–Labrador Shelf for the 1985-1987 period.....	33

## LIST OF FIGURES

Figure 1.	Relationships of consumption, growth efficiency, ecotrophic efficiency, and proportion of unassimilated food between the inverse A2 and Ecopath models .....	34
Figure 2.	Relationships of diet composition for values with modified weights (matrix A) and for constrained values (matrix G) between the inverse A2 and Ecopath models .....	35
Figure 3.	Distribution of predation mortality (expressed by prey biomass, $\Sigma Pr_{X \rightarrow Y}/B_X$ ) on fish prey for the inverse A2 and Ecopath models .....	36
Figure 4.	Composition of main predators on small cod ( $\leq 35$ cm), small Greenland halibut ( $\leq 40$ cm), flounders, redfish, small demersal feeders, and capelin for the inverse A2 and Ecopath models .....	37
Figure 5.	Composition of main predators on sand lance, arctic cod, piscivorous small pelagic feeders, planktivorous small pelagic feeders, shrimp, and large crustaceans for the inverse A2 and Ecopath models .....	38
Figure 6.	Composition of main predators on echinoderms, polychaetes, other benthic invertebrates, large zooplankton ( $> 5$ mm), and small zooplankton ( $< 5$ mm) for the inverse A2 and Ecopath models .....	39
Figure 7.	Composition of predation mortality (flux in $t\ km^{-2}\ yr^{-1}$ ) on small demersal feeders, large crustacea, and shrimp for the Ecopath and inverse A2 models .....	40

## LIST OF APPENDICES

Appendix 1. Diet Matrix for inverse modelling .....	41
Appendix 2. A simple three-compartment example of the inverse solution process.....	47
Appendix 3. Average and standard deviation of terms with large variability (SD > mean; in t km <sup>2</sup> yr <sup>-1</sup> ) for each inverse model.....	53
Appendix 4. Consumption by each group estimated by the inverse A2 model.....	54
Appendix 5. Diet composition of large cod, small cod, and small Greenland halibut estimated by the inverse A2 model.....	55
Appendix 6. Summary of the number of estimates that were at the limit set by the constraints for different parameters in the inverse A2 solution .....	56



## ABSTRACT

Savenkoff, C., A.F. Vézina, and A. Bundy. 2001. Inverse analysis of the structure and dynamics of the whole Newfoundland–Labrador Shelf ecosystem. *Can. Tech. Rep. Fish. Aquat. Sci.* 2354: viii+56 p.

In the present study, we use inverse methods to reconstruct trophic flows through the whole Newfoundland–Labrador Shelf ecosystem (NAFO 2J3KLNO) for the 1985-1987 period. This was a period of relatively constant biomass for the major species prior to the groundfish stock collapses. The whole-system model of the Newfoundland–Labrador Shelf is divided into 31 functional groups or compartments from phytoplankton and detritus to marine mammals and seabirds, including harvested species of pelagic, demersal, and benthic domains. The results are compared with a mass balance model using the Ecopath approach with the same data set. Successful development of the suite of ecosystem models proposed for the Comparative Dynamics of Exploited Ecosystems in the Northwest Atlantic (CDEENA) program will provide powerful new tools to evaluate the impact of human and environmental factors in a variety of Atlantic shelf ecosystems.

## RÉSUMÉ

Savenkoff, C., A.F. Vézina, and A. Bundy. 2001. Inverse analysis of the structure and dynamics of the whole Newfoundland–Labrador Shelf ecosystem. *Can. Tech. Rep. Fish. Aquat. Sci.* 2354: viii+56 p.

Dans cette étude, nous utilisons les méthodes inverses pour représenter les flux trophiques de l'écosystème complet de la région de Terre-Neuve et du Labrador (divisions 2J3KLNO) pour la période 1985-1987. Les biomasses des principales espèces étaient relativement constantes pendant cette période avant l'effondrement des stocks de poissons de fond. L'écosystème de la région de Terre-Neuve et du Labrador a été divisé en 31 groupes ou compartiments trophiques depuis le phytoplancton et les détritux aux oiseaux et mammifères marins incluant les espèces commerciales des domaines pélagique, démersal et benthique. Nous avons comparé les résultats avec ceux estimés par un autre modèle d'équilibre de masse utilisant l'approche Ecopath et développé sur les mêmes données. Le succès de l'élaboration des modèles écosystémiques proposés par le programme 'Comparative Dynamics of Exploited Ecosystems in the Northwest Atlantic' (CDEENA) apportera de nouveaux outils scientifiques efficaces pour évaluer l'impact des facteurs humains et environnementaux dans différents écosystèmes de l'Atlantique.

## PREFACE

This work was supported by a multidisciplinary and inter-regional program known as CDEENA (Comparative Dynamics of Exploited Ecosystems in the Northwest Atlantic). CDEENA originally proposed a comparative analysis of changes in the structure and function of Northwest Atlantic shelf ecosystems to determine how these may have affected the productivity of living resources. To this end, CDEENA brought together the expertise of field scientists and modellers to: (1) describe the changes in time and space, (2) identify and fill critical data gaps in the knowledge base, and (3) develop models to investigate ecosystem-level hypotheses (i.e., environmental variation, predation, fishing effects) concerning changes in reproduction, mortality, growth, and feeding of cod and other species.

The ecosystems that will be studied are the Newfoundland and Labrador Shelf (NAFO 2J3KLNO), the northern Gulf of St. Lawrence (NAFO 4RS), the southern Gulf of St. Lawrence (NAFO 4T), the eastern Scotian Shelf (NAFO 4VsW), and the western Scotian Shelf (NAFO 4X). CDEENA focuses on three periods: (1) the 1970s, prior to the extension of jurisdiction (1977) and the subsequent recovery of some groundfish stocks in some of these areas; (2) the mid-1980s, the peak of the recovery and prior to the groundfish collapses of the early 1990s in virtually all areas; and (3) the present, where the collapsed groundfish stocks have failed to recover in most areas. The program will test the hypothesis that the failure of the collapsed fish stocks to recover in the 1990s is explained by changes in the ecosystems of the NW Atlantic (e.g., changes in trophic structure) driven by a combination of biological, fishing, and environmental variation that affected the recruitment of young stages, either through predation or competition for resources. In the present study, we evaluate the potential of inverse methods to estimate a balanced flow network and also compare flow networks calculated by Ecopath (Bundy *et al.* 2000) and inverse methods for a common data set to determine how much impact the solution method has on the construction of flow networks for the Newfoundland and Labrador Shelf ecosystem for the 1985-1987 period.

## INTRODUCTION

A comprehensive understanding of the structure, function, and regulation of major ecosystems is necessary to face the world's ever-growing environmental problems (Mann 1988; Pahl-Wostl 1993; Gaedke 1995). Mass-balance biomass models (Ecopath approach) are being used globally as an efficient and useful method to systematically describe ecosystems and to explore their properties (Christensen and Pauly 1993; Christensen 1995; Pauly and Christensen 1996). They are a simple approach to represent the complexity of an ecosystem and involve a mass-balance description of trophic interactions. The trophic food web is depicted by a number of compartments or functional groups to which all organisms are allocated and which are interconnected by fluxes of matter. To estimate the magnitude of these fluxes, measurements or estimates of major process rates such as consumption, respiration, production, and the release of dead organic matter are required for each living compartment, as well as quantitative information on the diet composition of the different groups.

The Ecopath approach uses mass balance principles to estimate flows (Polovina 1984; Christensen and Pauly 1992). Each group is represented by one balanced equation and requires six input parameters: biomass (B), production (P), consumption (Q), ecotrophic efficiency (EE; the fraction of the production that is either passed up the food web or exported), diet composition, and catch of each group. The linear equations are solved via matrix algebra to produce estimates of the flows that balance inputs and outputs; any missing parameters are estimated (EE is estimated if all parameters have been entered). Export and diet composition must always be entered while of the four remaining basic input parameters (B, P, Q, and EE), three must be entered. In most cases, when all the information to run an Ecopath model is assembled, the model will not balance due to the inconsistencies in the information. In this case, the values of one or more of the terms can be changed iteratively until a balance is obtained. Indeed, there is more than one way to construct a Ecopath model and there is no unique solution to any model. However, where there are areas of the model that are well known and on which the modeller can place some certainty, then the number of plausible solutions is reduced. For the less certain parameters, sensitivity analysis can be used to examine their effects on the model. The ecotrophic efficiency provides an immediate check for mass balance (Christensen and Pauly 1992). If the model is not balanced, then there are negative flows to the detritus and ecotrophic efficiencies (EE) are greater than one. Arriving at a balanced network with the Ecopath approach is left largely to trial and error, either through user intervention or Monte-Carlo simulations.

Another approach to solving for the flows is to compute the solution that minimizes the imbalances between inputs and outputs. This inverse approach provides a global criterion for an optimal (balanced) solution (Parker 1977; Enting 1985; Vézina and Platt 1988; Vézina and Pace 1994; Vézina and Savenkoff 1999; Vézina *et al.* 2000). When the system of equations is strongly underdetermined, additional constraints (inequality relations) must be added to constrain the range of possible solutions and thus to obtain a meaningful solution. Each flow must be non-negative. Further, the flows (consumption) or ratios of flows (metabolic and ecotrophic efficiencies) are assumed to fall within certain ranges. The mass-balance equations and the additional constraints reduce the potential range of flux values, and trophic flows are estimated using an objective least-

squares criterion for an optimal (balanced) solution. The mass balance is closed by residuals (inputs–outputs) instead of ecotrophic efficiencies as in the Ecopath approach.

In the present study, we evaluate the potential of inverse methods to estimate a balanced flow network, if it exists, within the range of uncertainties in model parameters for the Newfoundland–Labrador Shelf for the 1985–1987 period. We also compare flow networks calculated by Ecopath (Bundy *et al.* 2000) and inverse methods for a common data set to determine how much impact the solution method has on the construction of flow networks.

## MATERIALS AND METHODS

### DATA USED IN MODELLING

The data used for the inverse model were taken from the data used in the Ecopath model described in Bundy *et al.* (2000). This data set covers an area equivalent to the southern third of the Labrador Shelf, the northeast Newfoundland Shelf, and the Grand Bank (NAFO Divisions 2J3KLNO) out to the 1,000 m bottom contour, a total area of 495,000 km<sup>2</sup>. The central and northern parts of the Labrador Shelf are excluded because the commercial fishery in the area is relatively small and surveys in the area have been infrequent. The period covered by the analysis is 1985 to 1987. This was a period of relatively constant biomass for the major species. It is also a period for which the data on diets of demersal fish are most complete (Bundy *et al.* 2000).

Based on the classification of Bundy *et al.* (2000), the whole-system model of the Newfoundland–Labrador Shelf is divided into 31 functional groups or compartments (Table 1). Species groups were defined on the basis of their commercial significance and importance as predators or prey. Atlantic cod (*Gadus morhua*), Greenland halibut (*Reinhardtius hippoglossoides*), and American plaice (*Hippoglossoides platessoides*) were each separated into two groups based on diet, age/size at first capture, and age/size at maturity. Smaller animals prey mainly on invertebrates and larger animals prey mainly on fish. These changes tend to occur gradually with increasing length, but for this model it was assumed that the change occurs at 35 cm for Atlantic cod and American plaice and at 40 cm for Greenland halibut (Bundy *et al.* 2000). Data about species, biomass, consumption, catch (here equal to export), and diet composition are summarized in Tables 1 and 2 and Appendix 1, respectively. More information can be found in Bundy *et al.* (2000).

### MODEL STRUCTURE

All flows in the model are identified and described in Table 3 and the mass balance equations for all compartments are given in Table 4. For individual compartments, consumption ( $\Sigma Pr_{X \rightarrow Y}$ ) representing the input must balance the sum of the outputs consisting of, e.g., production, respiration ( $R_Y$ ), and egestion (detrital flow,  $Det_Y$ ) (i.e., the food web is in steady state). In the Labrador–Newfoundland model, it was assumed that there was no year-to-year change in biomass over the 1985–1987 time period and that emigration was zero (Bundy *et al.* 2000). Thus

production in this model is simply the biomass that is lost to natural mortality (predation [ $\Sigma Pr_{Y \rightarrow X}$ ], disease, and other natural causes of death [ $M0_Y$ ]) and fishing mortality (export,  $EX_Y$ ) (Table 4). For the phytoplankton group, the net (corrected for respiration) production ( $Prod_{PHY}$ ) must balance the sum of the outputs (phytoplankton mortality including egestion term,  $M0_{PHY}$ , and consumption of phytoplankton,  $\Sigma Pr_{PHY \rightarrow X}$ ). For the detritus group, the inputs (egestion [non-assimilated food,  $\Sigma Det_X$ ] and other natural causes of death [ $\Sigma M0_X$ ] for other groups) must balance the sum of the outputs (consumption of detritus,  $\Sigma Pr_{DET \rightarrow X}$ ). In this study, remineralization of detritus is neglected.

Some of the input data are introduced as additional compartmental mass balance equations (Table 4). These include values for primary production ( $P_{PHY}$ ), exports (catches,  $Exp_X$ ) out of the system (boundary fluxes), consumption ( $Q_Y$ ), and diet proportions ( $DC_{U \rightarrow Y}$ ) locally estimated from field studies or available only as point estimates (no variance estimates) (Appendix 1). This procedure provides us with the flexibility to compute approximations to these flows rather than treat them as fixed in the model. This yielded 238 equations (31 mass balances and 207 specified flows; Table 4) that had to be solved for 388 unknown flows (Table 3).

## MODEL CONSTRAINTS

The system of equations above is strongly underdetermined, so additional constraints had to be added to obtain a meaningful solution (Table 5). Each flow was taken to be non-negative. Further, the flows or ratios of flows (metabolic efficiencies) were assumed to fall within certain ranges. Gross growth efficiency (GE) is the ratio of production to consumption and for most groups should have values between 0.1 and 0.3 (Christensen and Pauly 1992). Exceptions are top predators, e.g., marine mammals and seabirds, which can have lower GE, and small, fast growing fish larvae or nauplii or bacteria, which can have higher GE (Christensen and Pauly 1992; Table 5). Following Winberg (1956), 80% of the consumption was assumed to be physiologically useful for carnivorous fish groups if other estimates were not available while the non-assimilated food (20% consisting of urine and feces) was directed to the detritus. For herbivores, the proportion not assimilated could be considerably higher, e.g., up to 40% in zooplankton (Christensen and Pauly 1992). We constrained the assimilation efficiency (AE) to fall between 70 and 90% for all the groups except for large and small zooplankton (between 50 and 90%) (Table 5).

The consumption values not locally estimated from field studies or from literature reports were used as constraints (Table 5). The diets with reasonable estimates of uncertainty (SD greater than 0.6%) were also specified as constraints (Appendix 1). To facilitate comparisons with the Ecopath model, we added constraints on the ecotrophic efficiency (EE). The ecotrophic efficiency is the fraction of the production that is either passed up the food web or exported. These values should be between 0 and 1 (Christensen and Pauly 1992). Here, a value only slightly above zero indicates that the group is not consumed in noticeable amounts by any other group in the system (e.g., top predators). Conversely, a value near or equal to 1 indicates that the group is being heavily preyed upon and/or that fishing pressure is high, leaving no individuals to die of other causes (small prey organisms). Generally, an upper limit equal to 0.95 was used. This reflects the fact that in marine ecosystems most of the production is used for predation or fisheries

(Christensen and Pauly 1992, 1998). In all, 784 constraints were added to the 238 mass balance relations, leading to a system of 1022 equations to be solved for the 388 unknowns.

## MODEL SOLUTION

Details of the solution method for these equations are given in Vézina and Platt (1988), Vézina and Pace (1994), and Vézina and Savenkoff (1999). A simple example of the solution process is also provided in Appendix 2. Briefly, the mass balance and constraint equations are collected into matrix form:

$$\mathbf{S}^{-1/2} \mathbf{A} \mathbf{W}^{1/2} \mathbf{x} = \mathbf{S}^{1/2} \mathbf{b} \quad (1)$$

$$\mathbf{G} \mathbf{W}^{1/2} \mathbf{W}^{1/2} \mathbf{x} \geq \mathbf{h} \quad (2)$$

where  $\mathbf{A}$  contains the coefficients and  $\mathbf{b}$  contains the right-hand sides of the mass balance equations (Tables 2 and 4),  $\mathbf{G}$  contains the coefficients and  $\mathbf{h}$  the right-hand sides of the constraint equations (Tables 2, 3, and 5; Appendix 1), and  $\mathbf{S}$  and  $\mathbf{W}$  are the variance matrices of  $\mathbf{A}$  and  $\mathbf{x}$ , respectively. These equations are solved in four steps: (1) computation of an initial solution to Eq. 1 using singular value decomposition, (2) elimination of the mass balance constraints by projecting Eq. 2 on the null space of Eq. 1 (Vézina and Platt 1988), (3) solution of the transformed Eq. 2 using quadratic programming, and (4) addition of the solution of step 3 to the initial solution to obtain the final constrained solution. If this procedure failed to provide a reasonable solution, for example, with all flows nonnegative, then the highest orthogonal modes of Eq. 1 were successively removed until a solution was found (Vézina and Platt 1988). The solution process generates the simplest flow network that satisfies both the mass conservation and biological constraints. These operations were done with a Matlab® program that can be obtained from the authors.

One important part of the solution process is the choice of row and column weights. In this study, we used the variances of the observations (weights of the mass balance equations, row weights, which make up the diagonal of matrix  $\mathbf{S}$ ) and the variances of the unknown flows (weights of the unknown flows, column weights, which make up the diagonal of matrix  $\mathbf{W}$ ) (see Tables 3 and 4). The weights of the additional equations for groups with no information on parameter variability are the average of all known coefficients of variation for consumption ( $CV(Q_Y)_{\text{mean}} = 87\%$ ) and diet proportion ( $CV(DC_{U \rightarrow Y})_{\text{mean}} = 120\%$ ) to give them initially less weight in the solution.

In general, several orthogonal modes of Eq. 1 had to be removed to obtain a solution. Consequently, the solutions calculated for this study were not balanced, that is, the sum of the inputs and outputs for each compartment did not necessarily equal zero and the specified values were not reproduced exactly. These differences are here termed the residuals. We tested various model structures in trying to arrive at the smallest possible residuals. The best solutions were those that produced the smallest sums of squared residuals for the compartmental mass balances.

## NOISE IN THE DATA: SENSITIVITY STUDIES

To assess the solution's robustness to variations in the data, we applied random perturbations to the right-hand sides of the mass balance equations (vector **b**) (Table 4). We randomly perturbed each element of vector **b** by up to 10% (**b** replaced by  $[\mathbf{b} + r_n 0.1 \mathbf{b}]$ , where  $r_n$  is a randomly chosen real number between  $-1$  and  $1$ ; 10 random perturbations). For each model presented in the next section, the solutions are the means of 11 inversions corresponding to the 10 random perturbations (including a solution where  $r_n = 0$ ) on vector **b**. The elements of the vector **b** for the compartmental mass balance equations and the additional equations related to diet proportions are all equal to 0 (Table 4). Only the additional equations related to consumption, export, and primary production are equal to local measurements and thus can be randomly perturbed. In other modelling techniques,  $\pm 10\%$  random perturbations are also applied to the input data. Here, most of the input data (primary production, export, consumption, and diet) already have a large range of variability (coefficient of variation  $> 20\%$ ; see Table 2 and Appendix 1) that is used to constrain them.

## RESULTS

### SENSITIVITY OF INVERSE SOLUTIONS

Two inverse models were compared with the row and column weights described above: model A1 with initial weights and model A2 with modified weights for diet terms. The predation equations in model A2 were multiplied by a factor of 0.2 to give them less weight in the solution and thus to allow the model to increase the corresponding residuals. This was motivated by the prior belief that measurements of diets are uncertain, mostly representative of a key species for a functional group, and are not necessarily representative of the period and region investigated. The downweighting process left more room for the measured flows to change from their initially assigned values and thus allowed the model to potentially increase the imbalances between inputs and outputs.

The least-square mass balance residuals (normalized in inverse proportion to the weights of the mass balance equations to eliminate the effect of widely differing values among the parameters) indicated the compatibility (smallest overall sums of squared residuals) between inputs and outputs (Table 6). Model A2 had the smallest sums of squared residuals for all the equations. The solutions of model A2 kept the compartmental flows in as perfect a balance as possible. It is interesting to note that the weaker weights of the diet equations in matrix **A**, specified to give them less weight in the solution, not only improved the sums of squared residuals for diet but also for all the other equations. The model was improved by leaving more room for the measured flows to change from their initially assigned values for the diet equation. The downweighted predation equations allowed more flexibility to balance the flow networks.

Comparisons between means and standard deviations over 11 inversions showed that more than 90% of the estimated mean flows were larger than their corresponding standard deviation for each model (Table 7), thus characterizing the robustness of each model. We considered that a flow

had a large variability if its standard deviation among perturbations overlapped zero ( $SD > \text{mean}$ ). Predation and mortality terms presented the largest variabilities relative to the mean flow estimates for each model (Table 7). The terms with large variabilities are summarized in Appendix 3. The number of mortality terms with large variabilities increased with the lower weights of the diet equations in model A2. For the model A2, we present the model estimates and the corresponding inputs used as additional equations or constraints for consumption by each group and three specific diet composition of large cod, small cod, and small Greenland halibut, which summarized the results for the other diets (Appendices 4 and 5). The solution should not have too many flows that are bound to either their upper or lower limits (“sticky constraints”). A large number of sticky constraints suggests that the optimum may not have been found and, in any case, that the solution is determined by the a priori bounds rather than by patterns in the data. The model estimates are all between the upper and lower limits. Even though the model estimates seemed close to the limits in Appendix 4, only three groups (i.e., capelin, echinoderms, and molluscs) of the 24 groups with upper and lower constraints were at the limit set by the constraints for consumption (sticky-constraint estimates). A summary of the number of estimates that were at the limit set by the constraints for different parameters is presented in Appendix 6. Overall, 20% of the estimates in the A2 solution were sticky-constraint estimates (versus 37% for the A1 solution). This suggests that the final solution, especially for A2, is not overly determined by the bounds that we supplied.

## COMPARISONS OF INVERSE SOLUTIONS

Differences between the solutions of models A1 and A2 were relatively minor and were much smaller than the range in solution allowed by the inverse model constraints (Table 8). The largest divergences among the solutions appeared with the consumption by the large pelagic feeders and the diet composition of skates. The consumption by large pelagic feeders increased from 0.04 to 0.10 t km<sup>-2</sup> yr<sup>-1</sup> with the modified weights of the diet equations in matrix **A** (Table 9). Among the other groups, the consumption by flounders, redfish, large demersal feeders, arctic cod, and shrimp showed slight differences ( $20\% < |(X_{A1}-X_{A2})/X_{A1}| < 36\%$ ) between the two inverse models (Table 9). For the other groups, differences were less than 13%.

Among the seventeen fractions of prey in skate diet, only three values showed differences higher than 20% ( $27\% < |(X_{A1}-X_{A2})/X_{A1}| < 47\%$ ) between the two inverse models (Table 10). The modified weights of the diet equations imply an increase in the proportion of small demersal feeders and polychaetes consumed by the skates while the fraction of redfish decreased (Table 10).

Given the small differences between models, and the fact that model A2 yielded the best mass balance and the smallest number of sticky-constraint estimates, we compare only the results of inverse A2 model with the Ecopath results for the same data.



## COMPARISONS WITH THE MASS BALANCE MODEL USING THE ECOPATH APPROACH

Using the Ecopath approach developed for the same data set, Bundy *et al.* (2000) described three models: (1) an unbalanced model, (2) model 1, where the model is balanced by allowing the model to estimate the biomass of some prey groups, and (3) model 2 (termed the Ecopath model hereafter), which is model 1 with further modifications to the skates and an apparent trophic triangle of large crustacea, small demersal feeders, and shrimp to make results conform better with what is known or hypothesized about the ecosystem.

### Comparisons of model solutions

The inverse A2 and Ecopath models are two balanced models that provide two syntheses of our current knowledge of predation, consumption, and productivity in the ecosystem exploited by the Newfoundland fishery in areas 2J3KLNO for the 1985-1987 period. Indeed, since the number of flows to be solved ( $n = 388$  in this case) exceeds the number of independent mass balance relations, the solution obtained for each model is not unique. We examined the question of whether there were any major differences between the solutions obtained from the ad hoc iterations used by Bundy *et al.* (2000) in the Ecopath approach and the statistically optimized solutions of the inverse approach used here.

The differences between the A2 and Ecopath solutions were much smaller than the range in solutions allowed by the inverse model constraints (Table 8). The discrepancies were small for the proportion of food not assimilated (GS) and for the ecotrophic efficiencies (EE) while the largest divergences among the solutions appeared with the consumption, growth efficiency, and diet parameters. Relationships between the inverse A2 and Ecopath solutions were highly significant for consumption ( $r = 0.93$ ,  $p < 0.001$ ,  $n = 29$ ), growth efficiency ( $r = 0.68$ ,  $p < 0.001$ ,  $n = 29$ ), and ecotrophic efficiency ( $r = 0.77$ ,  $p < 0.001$ ,  $n = 31$ ) (Fig. 1). For growth efficiency, the inverse solution generally gave higher estimates than the Ecopath solution (more values above the 1:1 line in Fig. 1). The estimated unassimilated fraction varied over the whole 10-30% range in model A2 while the unassimilated fraction was not varied in the Ecopath solution, although it could be. With the Ecopath approach, when the model is not balanced, the first step is to reduce the EEs to less than 1 for all the groups with  $EE > 1$  by entering a default value of 0.95 (Polovina 1984, Christensen and Pauly 1992). Different groups had thus an ecotrophic efficiency fixed at 0.95 in the Ecopath solution while the ecotrophic efficiencies estimated by inverse analysis tended to be more variable than Ecopath EEs (Fig. 1). This can be viewed as analogous to the problem of sticky constraints in optimization. The variability in EEs means that the solution space was more thoroughly explored with the inverse approach than with Ecopath. Finally, inverse estimates of efficiencies are in general more dispersed than Ecopath efficiencies.

For diet composition, we compared values with modified weights (weak weights in matrix A) and constrained values (lower and upper limits in matrix G) between the inverse A2 and Ecopath models (Fig. 2). Results were similar between the two models ( $r = 1.00$ ,  $p < 0.001$ ,  $n = 197$  for diets in matrix A;  $r = 0.98$ ,  $p < 0.001$ ,  $n = 93$  for diets in matrix G). Even though the

predation equations in model A2 were multiplied by a factor of 0.2 to give them less weight in the solution (and thus to allow the model to increase the corresponding residuals), these diet proportions showed little divergence between the inverse A2 and Ecopath models (Fig. 2).

### Comparisons of ecotrophic efficiency

The ecotrophic efficiencies provided qualitatively the same information in the two models. These values were slightly above zero for marine mammals and seabirds, and fish were on average consumed heavily in the system ( $EE = 0.65 \pm 0.24$  and  $0.78 \pm 0.24$  for the inverse A2 and Ecopath models, respectively), with the exception of large cod ( $> 35$  cm), large Greenland halibut ( $> 40$  cm), large and small American plaice, and skate groups, for which the EE values were lower (between 0.19 and 0.62) (Table 9). However, the major divergences were in the EE of the small zooplankton, phytoplankton, and detritus groups. Indeed, the EE of small zooplankton indicated that 95% of their production was used in the system for the Ecopath model while the small zooplankton production was not fully used within the system for the inverse model A2 ( $EE = 0.40$ ; Table 9). The ecotrophic efficiency of phytoplankton in the Ecopath model was low ( $EE = 0.31$ ), showing only partial utilization of the phytoplankton, while 66% of the system's phytoplankton production was used for the inverse A2 model.

The ecotrophic efficiency of the detritus group is defined as the ratio between what flows out of that group and what flows into it. Under the steady-state assumption, this ratio should be close to one and was in the present study for inverse modelling. Thus, the detritus is completely recycled in the model (versus only 59% for the Ecopath model). The EE of detritus less than one for the Ecopath model implies that more is entering the detritus group than is exiting. The difference is assumed to end up as accumulated detritus, i.e., to be buried as sediment.

### Comparisons of mortality processes

The distribution of mortality processes (fishing mortality [= Exp here] and natural mortality [predation:  $\Sigma Pr_{Y \rightarrow X}$  or M2; disease and other natural causes of death: M0]) across the different groups is shown for each model in Table 11. Even though some divergences exist between the two models (seabirds, skates, small demersal feeders, and large pelagic feeders; see Table 11), the distributions of total mortality were very highly correlated ( $r = 1.00$ ,  $n = 30$ ,  $p < 0.001$ ). The total mortality for seabirds, skates, small demersal feeders, and large pelagic feeders was higher with the inverse A2 model. These divergences are related to changes in the absolute values of other natural causes of death for seabirds, skates, and small demersal feeders and to changes in absolute values of predation mortality for large pelagic feeders between the two models.

Predation mortality largely dominated for small cod ( $\leq 35$  cm), small Greenland halibut ( $\leq 40$  cm), flounders, redfish, large demersal feeders, capelin, sand lance, arctic cod, piscivorous small pelagic feeders, planktivorous small pelagic feeders, shrimp, large crustaceans, and large zooplankton for each model (Table 11). Other natural causes of death dominated for marine mammals, seabirds, large cod ( $> 35$  cm), large Greenland halibut ( $> 40$  cm), large and small

American plaice, echinoderms, molluscs, and polychaetes for each model. Fishing greatly exceeded predation mortality on large cod, large Greenland halibut, and skates for each model (Table 11). These results confirm that the fishery has a large impact on large fish groups.

There were some major differences in mortality processes between the two models. For skates, mortality by fishing dominated in the Ecopath model while other natural causes of death were the main mortality cause in the inverse A2 model (Table 11). For small demersal feeders, predation was the main mortality for the Ecopath model while predation mortality and other natural causes of death were relatively similar in the inverse A2 model. For large pelagic feeders, fishing mortality dominated for the Ecopath model and predation greatly exceeded fishing for the A2 model. For other benthic invertebrates and phytoplankton, other natural causes of death were the main cause of mortality for the Ecopath model while predation dominated in the inverse A2 model. Finally, predation greatly exceeded other natural causes of death for small zooplankton in the Ecopath solution while the result was reversed for the inverse A2 model. Although some divergences existed between the two models, relationships between each mortality process estimated by the inverse and Ecopath models were highly correlated (for export mortality: Spearman's  $r = 0.97$ ,  $n = 19$ ,  $p < 0.001$ ; for predation mortality: Spearman's  $r = 0.99$ ,  $n = 25$ ,  $p < 0.001$ ; for other natural causes of death: Spearman's  $r = 0.82$ ,  $n = 30$ ,  $p < 0.001$ ). Even though there was no direct constraint on mortality parameters (each model could change these terms without modifying the mass balance), these results showed a good robustness of mortality processes estimated by the two flow networks. The results showed also that different groups had a high degree of unexplained mortality (high percentage of other natural causes of death, e.g., large cod, large Greenland halibut, small American plaice; see Table 11). This might be caused by unreported discarding or dumping (unaccounted fishing mortality). Diseases, which were not monitored, could have also contributed to the unaccounted mortality.

### Comparisons of predation mortality

There are several key predators in this system. The mortality accounted for by the top vertebrate predators is shown in Table 12 for all prey and in Figure 3 for vertebrate prey. The distributions of predation mortality on all prey were correlated between the two models ( $r = 0.81$ ,  $n = 24$ ,  $p < 0.001$  for the ranks). In terms of overall predation, the top five predators (excluding invertebrate predators) were capelin, harp seals, large cod, fishing, and whales, respectively, in the Ecopath model. In the inverse A2 model, large cod are the top predators in the system followed by harp seals, small demersal feeders, capelin, and fishing. Capelin and fishing have relatively similar total predation for the two models, but the total predation values by large cod, harp seals, and small demersal feeders were higher in the inverse model. The same groups comprised the lowest three predators (seabirds, shrimp, and large pelagic feeders) in each model, but values and ranks differed (Table 12).

For predation on fish prey only, harp seals were the top predator in the system according to the Ecopath model (Fig. 3). Fishing, large cod, and whales were the greatest predators of fish after harp seals. The same key predators were present in the inverse A2 model, but they appeared in a different order (Fig. 3): harp seals, large cod, fishing, and whales. However, large cod, harp seals,

and whales accounted for at least 43% of the total mortality caused by vertebrate predators and fishing on fish in each model. The fishery represented 10% of total fish mortality in the inverse model A2 (versus 14% in the Ecopath model). For the two models, the fishery had a large impact on several species, including key commercial species such as large cod, large Greenland halibut, and large American plaice, but also other species such as skates, large pelagic feeders, and redfish. The fishery focuses on the large fish groups, the predators on the smaller fish.

The composition of predation mortality on certain individual prey groups for each model is shown in Figs. 4-6. The large cod and the large Greenland halibut were consumed by the harp and hooded seals only (not shown). The harp and hooded seals were also the two major predators of small Greenland halibut and flounders (Fig. 4). The harp seals had the largest predation pressure on Arctic cod (Fig. 5) and large pelagic feeders (not shown). The results showed that large cod ( $> 35$  cm) and harp seals were the two major predators of small cod ( $\leq 35$  cm) (Fig. 4). Large cod was also a major predator of small American plaice ( $\leq 35$ cm; not shown), small demersal feeders, capelin, and large crustaceans (Figs. 4 and 5). In the pelagic domain, there were small differences between the two models in the composition of the main predators. Capelin exerted a large predation pressure on sandlance in the Ecopath model while it was negligible in the inverse A2 model. Small demersal feeders exerted a larger predation pressure on shrimp in the inverse A2 model than in the Ecopath model (Fig. 5). In fact, small demersal feeders played a larger role in the predation of different prey groups in the inverse A2 model for the pelagic domain (see arctic cod, piscivorous small pelagic feeders, and large crustaceans in Fig. 5) in comparison to the Ecopath model. This is more obvious for the benthic domain, where small demersal feeders were the major predators of benthic invertebrates in the inverse A2 model (Fig. 6), surpassing the predation pressure by large crustaceans on these groups (Fig. 6).

However, there were some large quantitative differences between the two models in the total predation or predation fluxes on potential preys (Figs. 4-6 and Table 12). For example, total predation by large cod was higher by a factor of close to two (Table 12) and accordingly, large cod exerted a larger predation pressure on small cod in the inverse model than the Ecopath estimates (Fig. 4). These differences reflected an increased consumption (2 times) by large cod as estimated in the inverse solution (Table 9;  $8.87 \text{ t km}^{-2} \text{ yr}^{-1}$  versus  $4.50 \text{ t km}^{-2} \text{ yr}^{-1}$  in the Ecopath solution). The Ecopath model estimated a consumption by large cod close to the lower constraint limit while the inverse estimate was in the middle of the range (constraint limits between 4.44 and  $13.31 \text{ t km}^{-2} \text{ yr}^{-1}$ ).

Comparisons between specific assumptions to balance the Ecopath model and the inverse solution

Bundy *et al.* (2000) made several assumptions to balance the Ecopath model. More specifically, further data modifications to the skates and an apparent trophic triangle of large crustacea, small demersal feeders, and shrimp were made to force the Ecopath model to better conform to what is known or hypothesized about the ecosystem. We will specifically discuss below how the inverse model deals with these findings below.

### *Impact of skates*

The skate diet was originally adapted from the aggregate diet for larger thorny skates. The larger thorny skates eat more fish than smaller thorny skates, which feed mainly on cephalopods, polychaetes, and amphipods (Bundy *et al.* [2000] and corresponding references therein). Other skate species are also less piscivorous than the thorny skate. To allow for this, the proportion of fish in the diet was reduced by 20% and distributed over the polychaetes and amphipods (large zooplankton) by their relative contribution to the diet for the best Ecopath model. In the inverse model, the diet composition of skates was constrained by lower and upper values based on the different potential diets described by Bundy *et al.* (2000). The diet composition of the skates estimated by the inverse model is shown in Table 10. Fishes composed 68.4% of the skate diet (versus 54.8% in the Ecopath model), i.e., an increase of 14%. Predation on small demersal feeders, capelin, and sand lance was increased with the inverse A2 model while the proportions of large crustaceans, polychaetes, and large zooplankton in the diet were reduced (Table 10). However, the consumption was similar in each model (close to the lower limit,  $0.74 \text{ t km}^{-2} \text{ yr}^{-1}$ ; Table 9). The increase in the proportion of fish in the diet for the inverse A2 model thus yields a balanced solution. This finding contradicts several assumptions made by Bundy and collaborators to balance their Ecopath model.

### *Large crustacea–small demersal feeders–shrimp trophic triangle*

Large crustacea and small demersal feeders prey on each other. Predation by large crustacea is much stronger than predation by small demersal feeders. Shrimp are prey to both groups; these groups form a trophic triangle. This mutual predation drives the first two Ecopath models to estimate high biomasses for both large crustacea and small demersal feeders as the consequent high consumption of shrimp drives the biomass of this group upwards. Ecopath is a top-down modelling system; the model estimates are thus determined by the biomass and consumption rates of the top predators. After different changes in the diet composition for the large crustacea and for some of their predators, the biomass for the small demersal feeders required to balance the Ecopath model was ten times the original estimate (from  $0.23$  to  $2.38 \text{ t km}^{-2}$ ). For the shrimp and large crustaceans, the estimated biomasses were respectively four and ten times greater than the original estimates (from  $0.20$  to  $0.82 \text{ t km}^{-2}$  for the shrimp and from  $0.19$  to  $1.73 \text{ t km}^{-2}$  for the large crustaceans). Finally, in the final Ecopath model, no small demersal feeders in the diet of the large crustacea (no trophic flux in Fig. 7) were needed to balance the solution. Large cod and skates were the major predators of large crustacea while large crustacea and large cod had the highest consumption values of shrimp in the Ecopath solution (Fig. 7). For small demersal feeders, large cod and harp seals were the major predators in the Ecopath solution (Fig. 7).

In the inverse A2 model, the predation on large crustacea by skates was similar to the value estimated in the Ecopath model while the consumption by large cod and small demersal feeders increased (Fig. 7). For shrimp, large cod and small demersal feeders were the major predators in the inverse A2 model. Large cod had the largest predation value on small demersal feeders in the inverse A2 model, but large crustacea also had a high predation impact on small demersal feeders in the inverse solution. In fact, the inverse modelling increased the predation impact of large cod

and small demersal feeders on the large crustacea–small demersal feeders–shrimp trophic triangle. These results are related to differences in consumption values between the two models. By comparisons with the values estimated by the Ecopath model, the consumption by shrimp and large crustaceans were slightly reduced while those of small demersal feeders and large cod increased by a factor close to four in the inverse A2 model (Table 9). The inverse modelling thus gave a balanced solution using the constrained consumption ranges without largely modifying biomass and diet inputs (smallest overall sums of squared residuals).

## DISCUSSION

### VALIDITY OF MASS-BALANCE SOLUTIONS

To understand the changes that have occurred in the shelf ecosystems of the northwest Atlantic, and to provide a basis for future management advice, the Comparative Dynamics of Exploited Ecosystems in the Northwest Atlantic (CDEENA) program proposed the development of models to investigate ecosystem-level hypotheses (e.g., environmental variation, predation, fishing effects). The overall hypothesis of CDEENA is that there are significant changes in the energy flow pattern in the ecosystems of the Northwest Atlantic between pre-collapse (1980s) and post-collapse (1990s) periods and these changes are consistent in the different ecosystems. To this end, CDEENA originally proposed to determine the relative effects of environmental variation, predation, and fishing, and their interactions, on the population dynamics of marine resources inhabiting shelf ecosystems of the Northwest Atlantic.

Ecopath is the most widely used software to synthesize biomass and energetic data and to develop flow networks. However, due to the fact that ecosystem-level information is never complete, the solution obtained is not unique. There is a need to use different approaches on the same data to ascertain the robustness of inferred differences between periods and among ecosystems. In this paper, we developed balanced inverse models equivalent to the Ecopath structure in the Newfoundland–Labrador Shelf for the 1985–1987 period.

Our inverse solutions are balanced and valid in that they represent logical mass balance implications of the observations made in the Newfoundland–Labrador Shelf. Since the number of flows to be solved ( $n = 388$  in this case) exceeded the number of independent mass balance relations ( $m = 238$ ), the solutions are not unique. The modelling results described above were based on several areas of uncertainty for different groups at the lower and higher trophic levels (see Bundy *et al.* 2000 for uncertainties in the data). These uncertainties are transmitted down the food web since all production and losses must be balanced for each group. A high consumption at the top of the food web requires high production at all lower levels. The additional constraints reduce the potential range of flux values. Given sufficient data, they enable a rigorous consistency of the different information used to quantify the flow diagram and allow “guestimates” of some fluxes that are particularly inaccessible to measurements (Gaedke 1995).

Even though other parameters also had uncertainty and variability allowed in their values, empirical diet data for many groups in the model were sparse or non-existent for the area and

period studied and were thus taken from the literature. However, even for groups with good diet data, there were also uncertainties, such as combining inshore and offshore diets, assuming that the diet for the 1980s was the same as during the 1990s, assuming that the diet for a key species is representative of the functional group, and attributing the proportion of “unidentified” in stomach content analysis to one group rather than to another. The uses of lower and upper limits to constrain values and the choice of row and column weights to give them more or less weight in the solution makes inverse modelling a flexible tool to quantify mass-balanced flow diagrams and trophic transfer efficiencies that are internally consistent.

We have noted that differences between the solutions of the inverse A2 and Ecopath models were much smaller than the range in solutions allowed by the inverse model constraints. These differences were, however, larger than those between the two inverse models (Table 8). The discrepancies between the inverse A2 and Ecopath solutions were small for the proportion of unassimilated food and for the ecotrophic efficiencies while the largest divergences among the solutions appeared with the growth efficiency, estimated consumption, and estimated diet parameters. Here, the inverse modelling results were compared to results from an Ecopath model that was balanced using an ad hoc iterative approach. A more appropriate comparison would be with the results of an optimized Ecopath model using the optimization routine Ecoranger, where minimum and maximum values and probability distributions can be assigned to input parameters. Unfortunately, these results were not available. However, the results presented here demonstrate that most differences between the results using the two approaches are relatively small. The inverse and Ecopath models could be used iteratively, each supplying the other with optimized solutions. The inverse model may well be useful to obtain a first balanced solution. It could supply Ecopath with first-cut diet compositions and efficiencies (metabolic and ecotrophic) using an objective least-squares criterion. The Ecopath model could then estimate the biomass of each group corresponding to these inputs and important ecological indices (see Table 13).

Another discrepancy between the two models is the estimated burial of detritus. Under steady-state assumption, the ecotrophic efficiency (EE) should be equal to one, and that is the case in the present study for inverse modelling. Thus, the detritus was completely recycled in this model while the EE of detritus less than one for the Ecopath solution (59%) implies that more was entering the detritus group than exiting. The total flow to the detritus (egestion and other natural causes of death for other groups;  $2362 \text{ t km}^{-2} \text{ yr}^{-1}$ ) in the Ecopath solution is 1.6 times greater than that estimated in the inverse A2 solution ( $1447 \text{ t km}^{-2} \text{ yr}^{-1}$ ). The difference between inputs and outputs for the detritus group is assumed to end up as accumulated detritus, i.e., to be buried as sediment. However, this flow of  $970.7 \text{ t km}^{-2} \text{ yr}^{-1}$  in the Ecopath solution, needed to balance the model, is 16 times greater than the estimated burial for the Gulf of St. Lawrence ( $59.4 \text{ t WW km}^{-2} \text{ yr}^{-1}$  or  $5.9 \text{ g C m}^{-2} \text{ yr}^{-1}$ ; Silverberg *et al.* 2000). The export of detritus also implies higher total fluxes (egestion and other natural causes of death for other groups) to the detritus with the Ecopath approach (Table 13). As shown by the EE of phytoplankton, 31% of the primary production is used within the system only; 69% is thus channelled into the detritus (versus 34% in the inverse A2 model) to balance the export of detritus in the Ecopath solution. This finding implies that the inverse model estimated a net primary production 28% lower than that estimated with the Ecopath solution (Table 13).

Global indices of ecosystem structure and function have different sensitivities to the method of flow estimation. The inverse model produced a noticeable increase in respiration flows and a sharp decline in detritus flows (Table 13). As a result, the gross efficiency was 40% higher with the inverse solution than with the Ecopath solution. This is achieved without changing the trophic structure significantly, i.e., the mean fishery trophic level, the trophic levels assigned to individual compartments, connectance, and omnivory were all very similar between the solutions. Therefore, the inverse method as applied in this ecosystem model appears to exploit the “breathing room” in transformation efficiencies to produce a more efficient system with lower total throughput.

## PREDATION AND TRANSFER EFFICIENCY IN THE NEWFOUNDLAND-LABRADOR SHELF FOR THE 1985-1987 PERIOD

We have noted that the inverse A2 and Ecopath models have minor divergences for consumption, diet composition, and predation mortality, but what are the implications of these differences on the trophic structure of the whole ecosystem of the Newfoundland-Labrador Shelf for the 1985-1987 period?

In the Newfoundland-Labrador Shelf for the 1985-1987 period, the high level of predation was supported by a large pelagic forage base, which included capelin, sand lance, Arctic cod, and planktivorous small pelagic feeders. Large zooplankton and small zooplankton feeders formed the basis of this forage network. Small and large zooplankton were the major consumers of phytoplankton, with 95 and 5% of the phytoplankton grazing in the inverse model (versus 81 and 19%, respectively, for the Ecopath model). The ecotrophic efficiency of phytoplankton indicates that 66% of the production was used in the system, showing a large utilization of the phytoplankton for the inverse A2 model (versus 31% for the Ecopath model; see Table 9).

Since large zooplankton exerted the largest predation pressure on small zooplankton (Fig. 6), the transfer of organic matter from its entry into the system (by primary production) to the upper trophic level of the food web went mainly through the large zooplankton for the two models. It is also interesting to note that the production of small zooplankton was not fully used within the system ( $EE = 0.40$ ) for inverse model while the EE of small zooplankton for the Ecopath model indicates that 95% of its production was used (Table 9). The inverse analysis is in better agreement with the generally accepted concept that the lower trophic web is largely a recycling loop with low transfer efficiency to the upper level (Michaels and Silver 1988; Moloney *et al.* 1991; Legendre and Le Fèvre 1995) than is the Ecopath analysis.

For each model, large zooplankton was highly utilized within the system (79 and 95% for inverse A2 and Ecopath models, respectively). In both models, capelin and planktivorous small pelagic feeders were the main predators of large zooplankton, and capelin had a non-negligible predation impact on the small zooplankton (Fig. 6). Capelin and planktivorous small pelagic feeders were thus the critical converters of energy produced at lower trophic levels to a form available to other fish, sea mammals, and sea birds in the Newfoundland-Labrador Shelf for the 1985-1987 period.



Another important group for the input of organic matter or energy into the food web was the detritus. Since the benthic invertebrates were the main consumers of detritus (56, 25, 11, and 6% of detritus consumption for echinoderms, molluscs, polychaetes, and other benthic invertebrates, respectively), detritus fate is a critical input to the benthic domain. Small demersal feeders and large crustaceans were the main predators of benthic invertebrates, but to different extents depending on the model. They are the major links between the benthic invertebrates and the upper trophic levels of the demersal and pelagic domains.

The inverse A2 model estimated a key role of predator played by small demersal feeders on all prey in the system. This high predation pressure was related to a consumption value by small demersal feeders at the upper limit of the constrained range in the inverse solution. This high predation by small demersal feeders mainly on benthic invertebrates implied that a higher production of benthic invertebrates was used within the system, as shown by the larger EE for these groups in the inverse solution as compared to the Ecopath solution (Table 9). However, the transfer efficiency of the benthic invertebrates to the next trophic level is variable ( $[P - M0] / Q = P \times EE / Q = GE \times EE$ ). Thus, an average of close to 5% of the energy consumed by benthic invertebrates was transferred to the next trophic level while an average of 18% of the energy consumed by large and small zooplankton was transferred to the next trophic level in the pelagic domain. In the Ecopath model, divergences between the benthic and pelagic domains were greater. Indeed, an average of 28% of the energy consumed by the large and small zooplankton was transferred to the next trophic level in the pelagic domain (versus 2% in the benthic domain).

## CONCLUSION

In the present paper, we developed inverse models equivalent to the Ecopath structure for the Newfoundland–Labrador Shelf for the 1985–1987 period, prior to the groundfish stock collapses. We compared the balanced solutions with Ecopath results (Bundy *et al.* 2000) to evaluate the robustness of estimated flow networks. Differences between the solutions of inverse and Ecopath models are much smaller than the range in solution allowed by the inverse model constraints. In general, inverse estimates of efficiencies (growth efficiency, unassimilated fraction, ecotrophic efficiency) are more dispersed than Ecopath efficiencies, allowing more flexibility to balance the flow networks. The inverse techniques could provide diet composition and efficiency estimates for each group using an objective least-squares criterion for an optimal (balanced) solution, and thus replace the process that iteratively changes values of one or more of the input terms until a balance is obtained in the Ecopath model.

Basically, the inverse and Ecopath models agree on the distribution of consumption, predation, and fishing mortality. The key predators in the system are harp seals, large cod, and whales for the two models. Fishing mortality has a large impact on large fish groups and greatly exceeds predation mortality on large cod, large Greenland halibut, and skates for each model. Prior to the groundfish stock collapses, large cod and harp seals were the two major predators of small cod. The high level of predation in this system is supported by a large pelagic forage base, which includes capelin, sand lance, Arctic cod, and planktivorous small pelagic feeders. The study confirms the basic role played by capelin in the transfer of energy from phytoplankton–

zooplankton to other fish, sea mammals, and sea birds. A discrepancy between the two models is the key predator role of small demersal feeders on all prey suggested by the inverse modelling. Small demersal feeders were the main predators of benthic invertebrates which were the main consumers of detritus. Small demersal feeders are thus the major links between the detritus–benthic invertebrates and the upper trophic levels of the demersal and pelagic domains in the inverse solution. The inverse method as applied here appears to exploit the “breathing room” in transformation efficiencies to produce a more efficient system (40% higher with the inverse solution than with the Ecopath solution) with lower total throughput and without changing the trophic structure significantly, i.e., the mean fishery trophic level, the trophic levels assigned to individual compartments, connectance, and omnivory were all very similar between solutions.

We plan to extend these approaches (Ecopath and inverse modelling) further to other Atlantic shelf ecosystems (northern and southern Gulf of St. Lawrence, eastern and western Scotian Shelf) for periods prior to and after the groundfish collapses of the early 1990s in virtually all areas. These powerful new tools could identify critical data gaps in the knowledge base and investigate ecosystem-level hypotheses (e.g., environmental variation, predation, fishing effects) concerning changes in reproduction, mortality, growth, and feeding of cod and other species.

## ACKNOWLEDGEMENTS

This study was carried out as a contribution to the Canadian CDEENA (Comparative Dynamics of Exploited Ecosystems in the Northwest Atlantic) program with financial support from the Department of Fisheries and Oceans, Canada (Science Strategic funds). This report is a contribution to the research programs of the Maurice Lamontagne Institute (Division of Ocean Sciences, Department of Fisheries and Oceans, Canada), and the Bedford Institute of Oceanography (Division of Coastal Ocean Science, Department of Fisheries and Oceans, Canada). Gratitude is extended to L. Devine for reading and commenting on the manuscript. We also thank Drs. M. Castonguay and B. Mohn for their comments and reviews of the manuscript.

## REFERENCES

- Bundy, A., G.R. Lilly, and P.A. Shelton. 2000. A mass balance model for the Newfoundland–Labrador Shelf. *Can. Tech. Rep. Fish. Aquat. Sci.* 2310: xiv + 157 p.
- Christensen, V. 1995. A model of trophic interactions in the North Sea in 1981, the Year of the Stomach. *Dana* 11: 1-28.
- Christensen, V., and D. Pauly. 1992. ECOPATH II—a software for balancing steady-state ecosystem models and calculating network characteristics. *Ecol. model.* 61: 169-185.
- Christensen, V., and D. Pauly (Editors). 1993. Trophic models of aquatic ecosystems. *ICLARM Conf. Proc.*, 26, 390 p.
- Christensen, V., and D. Pauly. 1998. Changes in models of aquatic ecosystems approaching carrying capacity. *Ecol. Applications* 8 (supplement): S104-S109.
- Enting, I.G. 1985. A classification of some inverse problems in geochemical modelling. *Tellus* 37B: 216-229.

- Gaedke, U. 1995. A comparison of whole-community and ecosystem approaches (biomass size distributions, food web analysis, network analysis, simulation models) to study the structure, function and regulation of pelagic food webs. *J. Plankton Res.* 17: 1273-1305.
- Legendre, L., and J. Le Fèvre. 1995. Microbial food webs and the export of biogenic carbon in oceans. *Aquat. Microb. Ecol.* 9: 69-77.
- Mann, K.H. 1988. Towards predictive models for coastal marine ecosystems, p. 291-316. *In*: L.R. Pomeroy and J.J. Alberts (eds.). *Concepts of Ecosystem Ecology*, Ecological Studies 67, Springer, New York.
- Michaels, A.F., and M.W. Silver. 1988. Primary production, sinking fluxes and the microbial food web. *Deep-Sea Res.* 35: 473-490.
- Moloney, C.L., J.G. Field, and M.I. Lucas. 1991. The size-based dynamics of plankton food webs. II. Simulations of three contrasting southern Benguela food webs. *J. Plankton Res.* 13: 1039-1092.
- Pahl-Wostl, C. 1993. Food webs and ecological networks across temporal and spatial scales. *Oikos* 66: 415-432.
- Parker, R.L. 1977. Understanding inverse theory. *Annual Review of Earth and Planetary Sciences* 5: 35-64.
- Pauly, D., and V. Christensen. 1996. Mass Balance Models of North-eastern Pacific Ecosystems. Fisheries Centre Research Reports, University of British Columbia, Canada, Vol. 4, 131 p.
- Pitt, T.K. 1973. Food of American plaice (*Hippoglossoides platessoides*) from the Grand Bank, Newfoundland. *J. Fish. Res. Board Can.* 30: 1261-1273.
- Polovina, J.J. 1984. Model of a coral reef ecosystem. The ECOPATH model and its application to French Frigate Shoals. *Coral Reefs* 3: 1-11.
- Silverberg, N., B. Sundby, A. Mucci, S. Zhong, T. Arakaki, P. Hall, A. Landén, and A. Tengberg. 2000. Remineralization of organic carbon in eastern Canadian continental margin sediments. *Deep-Sea Res. II*, 47: 699-731.
- Vézina, A.F., and M.L. Pace. 1994. An inverse model analysis of planktonic food webs in experimental lakes. *Can. J. Fish. Aquat. Sci.*, 51: 2034-2044.
- Vézina, A.F., and T. Platt. 1988. Food web dynamics in the ocean. I. Best-estimates of flow networks using inverse methods. *Mar. Ecol. Prog. Ser.* 42: 269-287.
- Vézina, A.F., and C. Savenkoff. 1999. Inverse modeling of carbon and nitrogen flows in the pelagic food web of the Northeast Subarctic Pacific. *Deep-Sea Res. II*, 46: 2909-2939.
- Vézina, A.F., C. Savenkoff, S. Roy, B. Klein, R. Rivkin, J.-C. Therriault, and L. Legendre. 2000. Export of biogenic carbon and structure and dynamics of the pelagic food web in the Gulf of St. Lawrence. II. Inverse analysis. *Deep-Sea Res. II*, 47: 609-635.
- Winberg, G.G. 1956. Rate of metabolism and food requirements of fish. *Fish. Res. Board Can. Transl. Ser.* 253.

Table 1. Functional groups used in inverse modelling for the 1985-1987 period in the Newfoundland–Labrador Shelf.

Group Name	code	Main species
Whales and porpoises	WHA	<i>Megaptera novaeangliae</i> , <i>Balaenoptera physalus</i> , <i>Balaenoptera acutorostrata</i> , <i>Balaenoptera borealis</i> , <i>Physeter catodon</i> , <i>Globicephala melaena</i> , <i>Balaenoptera musculus</i> , <i>Phocoena phocoena</i>
Harp seals	HAS	<i>Phoca groenlandica</i>
Hooded seals	HOS	<i>Cystophora cristata</i>
Seabirds	SEA	<i>Oceanodroma leucorhoa</i> , <i>Sula bassana</i> , <i>Larus delawarensis</i> , <i>L. argentatus</i> , <i>L. marinus</i> , <i>Rissa tridactyla</i> , <i>Sterna hirundo</i> , <i>S. paradisaea</i> , <i>Uria aalge</i> , <i>U. lomvia</i> , <i>Alca torda</i> , <i>Fratercula arctica</i>
Large cod (> 35 cm)	LCO	<i>Gadus morhua</i>
Small cod ( $\leq$ 35 cm)	SCO	<i>Gadus morhua</i>
Large Greenland halibut (> 40 cm)	LGH	<i>Reinhardtius hippoglossoides</i>
Small Greenland halibut ( $\leq$ 40 cm)	SGH	<i>Reinhardtius hippoglossoides</i>
Large American plaice (> 35 cm)	LAP	<i>Hippoglossoides platessoides</i>
Small American plaice ( $\leq$ 35cm)	SAP	<i>Hippoglossoides platessoides</i>
Flounders	FLO	<i>Limanda ferruginea</i> , <i>Glyptocephalus cynoglossus</i> , <i>Pseudopleuronectes americanus</i>
Skates	SKA	<i>Raja radiata</i> , <i>R. senta</i> , <i>R. ocellata</i> , <i>R. spinicauda</i> , <i>R. laevis</i>
Redfish	RED	<i>Sebastes mentella</i> , <i>Sebastes fasciatus</i>
Large demersal feeders	LDF	<i>Urophycis tenuis</i> , <i>Melanogrammus aeglefinus</i> , <i>Macrouridae</i> , <i>Anarhichas</i> spp., <i>Zoarcidae</i> , <i>Cyclopterus lumpus</i> , <i>Lophius americanus</i> , <i>Hippoglossus hippoglossus</i>
Small demersal feeders	SDF	<i>Pholidae</i> , <i>Stichaeidae</i> , <i>Lycodes</i> , <i>Lycenchelys</i> spp., <i>Cottidae</i> , <i>Agonidae</i> , <i>Cyclopteridae</i> , <i>Liparidae</i> , juvenile LDF
Capelin	CAP	<i>Mallotus villosus</i>
Sand lance	SLA	<i>Ammodytes dubius</i>

Table 1., cont.

Group Name	code	Main species
Arctic cod	ACO	<i>Boreogadus saida</i>
Large pelagic feeders	LPF	<i>Cetorhinus maximus</i> , <i>Squalus acanthias</i> , <i>Thunnus thynnus</i> , <i>Pollachius virens</i> , <i>Merluccius bilinearis</i> , <i>Xiphias gladius</i> , <i>Salmo salar</i>
Piscivorous small pelagic feeders	PISF	<i>Scomber scombrus</i> , piscivorous myctophids and other mesopelagics, <i>Illex illecebrosus</i> , piscivorous juvenile LPF
Planktivorous small pelagic feeders	PLSF	<i>Clupea harengus harengus</i> , planktivorous myctophids and other mesopelagics, <i>Scomberesox saurus</i> , <i>Gonatus</i> sp., planktivorous juvenile LPF
Shrimp	SHR	<i>Pandalus borealis</i>
Large crustaceans	LCRU	<i>Homarus americanus</i> , <i>Chionoecetes opilio</i> , other non-commercial species ( <i>Hyas</i> spp.)
Echinoderms	ECH	<i>Echinarachnius parma</i> , <i>Stronglyocentrotus pallidus</i> , <i>Ophiura robusta</i>
Molluscs	MOL	<i>Mesodesma deauratum</i> , <i>Cyrtodaria siliqua</i>
Polychaetes	POL	<i>Exogene hebes</i>
Other benthic invertebrates	OBİ	Miscellaneous crustaceans, nematodes, other meiofauna
Large zooplankton (> 5 mm)	LZOO	Euphausiids, chaetognaths, hyperiid amphipods, cnidarians and ctenophores (jellyfish), mysids, tunicates >5 mm, ichthyoplankton
Small zooplankton (< 5 mm)	SZOO	Copepods (mainly <i>Calanus finmarchicus</i> and <i>Oithona similis</i> ), tunicates < 5 mm, meroplankton
Phytoplankton	PHY	Diatom species such as <i>Chaetoceros decipiens</i> and <i>Thalassiosira</i> spp., dinoflagellates, nanoflagellates
Detritus	DET	

Table 2. Input parameters for inverse modelling estimated from Bundy *et al.* (2000). Group name abbreviations are defined in Table 1. B: biomass (t wet weight km<sup>-2</sup>), Q: consumption rate (t km<sup>-2</sup> yr<sup>-1</sup>), EX: exports (including catches) out of the system (t km<sup>-2</sup> yr<sup>-1</sup>). SD: standard deviation, Min: minimum, Max: maximum.

Group	B				Q				EX <sup>a</sup>
Name	Value	± SD	Min	Max	Value	± SD	Min	Max	
WHA	0.25	0.14 <sup>b</sup>			2.96	2.58 <sup>c</sup>			
HAS	0.18	0.10 <sup>b</sup>			3.20	2.79 <sup>c</sup>			9.00 x 10 <sup>-4</sup>
HOS	0.03	0.02 <sup>b</sup>			0.45	0.39 <sup>c</sup>			1.79 x 10 <sup>-4</sup>
SEA	0.01	0.01 <sup>b</sup>			0.66	0.57 <sup>c</sup>			1.00 x 10 <sup>-3</sup>
LCO	2.04	1.15 <sup>b</sup>			8.87	6.27	4.44	13.31	6.03 x 10 <sup>-1</sup>
SCO	0.22	0.17	0.09	0.34	1.48	1.83	0.19	2.78	
LGH	0.35	0.20 <sup>b</sup>			0.51	0.45 <sup>c</sup>			3.50 x 10 <sup>-2</sup>
SGH	0.33	0.24	0.17	0.50	1.40	1.18	0.56	2.23	2.00 x 10 <sup>-3</sup>
LAP	0.97	0.55 <sup>b</sup>			1.59	0.51	1.23	1.94	1.00 x 10 <sup>-1</sup>
SAP	0.78	0.44 <sup>b</sup>			2.93	1.04	2.20	3.66	2.50 x 10 <sup>-2</sup>
FLO	0.99	0.17	0.87	1.11	3.28	1.80	2.01	4.56	7.90 x 10 <sup>-2</sup>
SKA	0.39	0.18	0.26	0.52	1.12	0.53	0.74	1.49	3.70 x 10 <sup>-2</sup>
RED	1.43	0.64	0.98	1.88	2.85	1.27	1.95	3.75	1.78 x 10 <sup>-1</sup>
LDF	0.85	0.47 <sup>b</sup>			1.48	1.04	0.74	2.21	5.20 x 10 <sup>-2</sup>
SDF	2.64	3.42	0.23	5.06	10.20	14.20	0.15	20.24	
CAP	13.45	0.23	13.29	13.61	86.09	39.95	57.84	114.34	1.26 x 10 <sup>-1</sup>
SLA	2.40	0.42	2.10	2.69	18.38	13.00	9.19	27.57	
ACO	2.87	0.19	2.73	3.00	7.64	5.48	3.77	11.52	
LPF	0.03	0.02 <sup>b</sup>			0.08	0.05	0.04	0.12	6.00 x 10 <sup>-3</sup>
PISF	0.96	0.77	0.41	1.51	4.69	6.17	0.33	9.05	1.50 x 10 <sup>-2</sup>
PLSF	2.14	2.02	0.71	3.57	9.20	12.21	0.57	17.84	1.90 x 10 <sup>-2</sup>
SHR	0.51	0.43	0.20	0.82	7.34	9.24	0.81	13.87	4.00 x 10 <sup>-3</sup>
LCRU	0.96	1.09	0.19	1.73	3.95	5.43	0.11	7.79	1.60 x 10 <sup>-2</sup>
ECH	112.30	63.05 <sup>b</sup>			517.83	414.69	224.60	811.06	
MOL	42.10	23.64 <sup>b</sup>			217.75	194.82	79.99	355.51	3.00 x 10 <sup>-4</sup>
POL	10.50	5.89 <sup>b</sup>			199.50	212.84	49.00	350.00	
OBI	7.80	4.38 <sup>b</sup>			223.17	223.68	65.00	381.33	

Table 2., cont.

Group	B				Q				EX <sup>a</sup>
Name	Value	± SD	Min	Max	Value	± SD	Min	Max	
LZOO	20.40	2.91	18.34	22.46	767.63	947.25	97.83	1437.44	
SZOO	27.69	8.46	21.70	33.67	652.46	677.20	173.60	1131.31	
PHY	19.23	10.80	11.59	26.86					
DET	269.00	169.71	149.00	389.00					

<sup>a</sup>:  $EX_X = C_X + E_X$ , where  $C_X$  is the catch of group X and  $E_X$  is the coefficient for other exports (emigration out of the system, food intake of predators that are not part of the system, and sedimentation) of group X. Here, E is assumed to be equal to 0.

<sup>b</sup>: calculated as  $B_X * CV(B_Y)_{\text{mean}}$ , where  $CV(B_Y)_{\text{mean}} = 56\%$ , the average of all known coefficients of variation for biomass.

<sup>c</sup>: calculated as  $Q_X * CV(Q_Y)_{\text{mean}}$ , where  $CV(Q_Y)_{\text{mean}} = 87\%$ , the average of all known coefficients of variation for consumption.

Table 3. Unknown flows (388; in  $\text{t km}^{-2} \text{ yr}^{-1}$ ) and corresponding weights used in the inverse modelling. Var: variance, CV: coefficient of variation, B: biomass, Q: consumption, DC: proportion in diet (by mass).

Notation	Description	# unknowns	Weight
$R_X$	Respiration of group X <sup>a</sup>	29	$\text{Var}(B_X)$
$\text{Det}_X$	Flow of group X to detritus <sup>b</sup>	29	$\text{Var}(B_X)$
$M0_X$	Mortality (other than predation) of group X <sup>c</sup>	30	$\text{Var}(B_X)$
$\text{Pr}_{X \rightarrow Y}$	Predation of group X by group Y	280	$\text{Var}(\text{Pr}_{X \rightarrow Y}) = Q_Y^{2*} \cdot (\text{CV}(\text{DC}_{U \rightarrow Y})^2 + \text{CV}(Q_Y)^2)$
$\text{Exp}_X$	Exports (including catches) of group X out of the system <sup>d</sup>	19	$\text{Var}(B_X)$
$\text{Prod}_{\text{PHY}}$	Net primary production	1	$\text{Var}(P_{\text{PHY}})$

<sup>a</sup>: No respiration term for phytoplankton or detritus.

<sup>b</sup>: No egestion term for phytoplankton (included in mortality term) or detritus.

<sup>c</sup>: No mortality term for detritus.

<sup>d</sup>: No export term for several groups (see Table 2).



Table 4. Mass balance and additional equations and corresponding weights used in the inverse modelling. Symbols for groups and measured and estimated model flows are in Tables 1, 2, and 3, respectively. Var: variance, CV: coefficient of variation.

Mass		#	
balance for	Equation	Eq.	Weight
Consumers	$\Sigma \text{Pr}_{X \rightarrow Y} - R_Y - \text{Det}_Y - M0_Y - \Sigma \text{Pr}_{Y \rightarrow X} - \text{EX}_Y = 0$	29	$\text{Var}(B_Y)$
PHY	$\text{Prod}_{\text{PHY}} - M0_{\text{PHY}} - \Sigma \text{Pr}_{\text{PHY} \rightarrow X} = 0$	1	$\text{Var}(B_{\text{PHY}})$
DET	$\Sigma \text{Det}_X + \Sigma M0_X - \Sigma \text{Pr}_{\text{DET} \rightarrow X} = 0$	1	$\text{Var}(B_{\text{DET}})$
Primary prod	$\text{Prod}_{\text{PHY}} = P_{\text{PHY}}^a$	1	$\text{Var}(P_{\text{PHY}})$
Export <sup>b</sup>	$\text{Exp}_X = \text{EX}_X$	19	$\text{Var}(B_X)$
Consumption <sup>c</sup>	$\Sigma \text{Pr}_{X \rightarrow Y} = Q_Y$	6	$\text{Var}(Q_Y)$
Predation <sup>d</sup>	$\text{DC}_{U \rightarrow Y} * \Sigma \text{Pr}_{X \rightarrow Y} - \text{Pr}_{U \rightarrow Y} = 0$	181	$\text{Var}(\text{Pr}_{X \rightarrow Y}) = Q_Y^{2*}$ $(\text{CV}(\text{DC}_{U \rightarrow Y})^2 + \text{CV}(Q_Y)^2)$

<sup>a</sup>:  $P_{\text{PHY}} = 1790 \text{ t km}^{-2} \text{ yr}^{-1}$  (net production).

<sup>b</sup>:  $\text{EX}_X$  is the estimate of  $\text{Exp}_X$  (see Table 2).

<sup>c</sup>: Only consumption values for the WHA, HAS, HOS, SEA, LCO, and LGH groups are used here (see Table 2).

<sup>d</sup>: Only diets without SD or with  $\text{SD} < 0.6\%$  (see Appendix 1). Note that the weight of the additional diet equations for groups with no information on diet proportion variability is the average of all known coefficients of variation for diet proportion ( $\text{CV}(\text{DC}_{U \rightarrow Y})_{\text{mean}} = 120\%$ ).

Table 5. Constraints on food web processes used in the inverse modelling.

# Eq.	Description of constraint	Equation
<u>Non-Negativity</u>		
1-388	All the unknown flows are nonnegative	$R_X \geq 0$
		$Det_X \geq 0$
		$M0_X \geq 0$
		$Pr_{X \rightarrow Y} \geq 0$
		$Exp_X \geq 0$
		$Prod_{PHY} \geq 0$
<u>Growth efficiency</u>		
389-446	Growth efficiency (of food conversion; GE = P/Q) ranges between: 0.1-1% for marine mammals and seabirds; 10-30% for fish, shrimp, large crustaceans, and large zooplankton; 9-30% for benthic invertebrates; 25-50% for small zooplankton	$GE_y^{\min} < \frac{\sum_x Pr_{x \rightarrow y} - R_y - D_y}{\sum_x Pr_{x \rightarrow y}} < GE_y^{\max}$
<u>Assimilation efficiency</u>		
447-504	Assimilation efficiency (AE) ranges between 70 and 90% for all the groups except for large and small zooplankton (50-90%)	$AE_y^{\min} < \frac{\sum_x Pr_{x \rightarrow y} - D_y}{\sum_x Pr_{x \rightarrow y}} < AE_y^{\max}$

Table 5., cont.

# Eq.	Description of constraint	Equation
	<u>Ecotrophic efficiency</u>	$EE_y^{\min} < \frac{\sum_x Pr_{x \rightarrow y} - R_y - D_y - MO_y}{\sum_x Pr_{x \rightarrow y} - R_y - D_y} < EE_y^{\max}$
505- 564	Ecotrophic efficiency (EE: production exported or consumed within the system) ranges between 0-0.95 for all groups except: Detritus: no constraint; Marine mammals: 0-0.10; Seabirds: 0-0.40	
	<u>Consumption</u>	$Q_y^{\min} < \sum_x Pr_{x \rightarrow y} < Q_y^{\max}$
565- 610	Predation of group X by group Y ranges between minimum and maximum consumption values (see Table 2)	
	<u>Predation</u>	$DC_{u \rightarrow y}^{\min} < \frac{Pr_{u \rightarrow y}}{\sum_x Pr_{x \rightarrow y}} < DC_{u \rightarrow y}^{\max}$
611- 784	Proportion of prey X in diet (by mass) of consumer Y ranges between minimum and maximum values (see Appendix 1)	

Table 6. Sums of squared normalized (divided by weights, diagonal of matrix **S**) residuals for the compartmental mass balances. A1: diet model with initial weights, A2: model with modified weights for diet terms.

Equations in A	A1	A2
All	$1.5 \times 10^{-3}$	$1.2 \times 10^{-6}$
Mass Balance	$2.0 \times 10^{-7}$	$3.1 \times 10^{-12}$
Export	$2.0 \times 10^{-7}$	$3.1 \times 10^{-12}$
Consumption	$1.4 \times 10^{-3}$	$1.5 \times 10^{-11}$
Diet	$1.4 \times 10^{-5}$	$1.2 \times 10^{-6}$
Primary production	$1.6 \times 10^{-13}$	$1.6 \times 10^{-13}$

Table 7. Number of mean flow estimates (averaged over 11 inversions) that are described as small variability (mean > SD) or large variability (mean < SD), and details of large variability terms (last three columns). The mean of the different coefficients of variation (CV = SD/mean) for all the terms is also shown. A1: initial model, A2: model with modified weights for diet terms.

Model	Small variability terms	CV Mean	Large variability terms	Near-zero (e.g., $10^{-14}$ - $10^{-20}$ ) terms	Predation terms	Mortality terms
A1	369 / 388 <sup>a</sup>	27%	19 / 388	7 / 19	9 / 19	3 / 19
A2	366 / 388	26%	22 / 388	4 / 22	9 / 22	9 / 22

<sup>a</sup>: Of the 388 unknowns, model A1 estimated 369 mean flows that were larger than their standard deviations (mean > SD).

Table 8. Root mean square difference (RMSD) obtained between the minimum and maximum constraints, between the A1 and A2 models, and between the inverse A2 and Ecopath models on each flow/efficiency. Q: consumption, GS: proportion of food not assimilated, GE: growth efficiency, EE: ecotrophic efficiency; Diet: diet component as a proportion of consumption.

Flow/efficiency	RMSD between constraints	RMSD between A1 and A2 models	RMSD between A2 and Ecopath models
Q	372	4	103
GS	0.22	0.03	0.06
GE	0.19	0.03	0.09
EE	0.89	0.09	0.23
Diet	0.09	0.01	0.03

Table 9. Consumption and ecotrophic efficiency estimated from inverse and Ecopath modelling. A1: model with initial weights, A2: model with modified weights for diet terms, Ecopath: model of Bundy *et al.* (2000). See Table 1 for group name meanings.

Group	Consumption ( $\text{t km}^{-2} \text{ yr}^{-1}$ )				Ecotrophic efficiency (dimensionless)			
	Constrained range	A1	A2	Ecopath	Constrained range	A1	A2	Ecopath
WHA	2.96	2.96	2.96	2.96	0-0.10	0.00	0.00	0.00
HAS	3.20	3.20	3.20	3.20	0-0.10	0.03	0.03	0.05
HOS	0.45	0.45	0.44	0.45	0-0.10	0.04	0.05	0.00
SEA	0.66	0.64	0.66	0.66	0-0.40	0.16	0.15	0.33
LCO	4.44-13.31	8.87	8.87	4.50	0-0.95	0.42	0.42	0.52
SCO	0.19-2.78	1.62	1.62	1.67	0-0.95	0.95	0.95	0.95
LGH	0.51	0.51	0.51	0.51	0-0.95	0.46	0.43	0.62
SGH	0.56-2.23	2.07	1.93	2.11	0-0.95	0.75	0.76	0.95
LAP	1.23-1.94	1.91	1.82	1.94	0-0.95	0.27	0.31	0.19
SAP	2.20-3.66	3.52	3.32	2.93	0-0.95	0.29	0.35	0.46
FLO	2.01-4.56	2.01	2.74	3.93	0-0.95	0.71	0.60	0.95
SKA	0.74-1.49	0.74	0.77	0.74	0-0.95	0.19	0.21	0.53
RED	1.95-3.75	3.05	2.28	3.20	0-0.95	0.60	0.80	0.95
LDF	0.74-2.21	0.74	0.96	1.48	0-0.95	0.86	0.80	0.68
SDF	0.15-20.24	17.69	19.49	4.76	0-0.95	0.67	0.47	0.95
CAP	57.84-114.34	57.80	57.80	57.14	0-0.95	0.95	0.94	0.85
SLA	9.19-27.57	9.19	10.08	17.71	0-0.95	0.93	0.81	0.95
ACO	3.77-11.52	3.77	4.56	7.39	0-0.95	0.95	0.78	0.95
LPF	0.04-0.12	0.04	0.10	0.10	0-0.95	0.95	0.95	0.95
PISF	0.33-9.05	3.47	3.53	2.48	0-0.95	0.89	0.86	0.95
PLSF	0.57-17.84	17.80	15.52	10.56	0-0.95	0.84	0.67	0.95
SHR	0.81-13.87	4.65	5.59	7.89	0-0.95	0.95	0.95	0.95
LCRU	0.11-7.79	5.97	5.79	7.66	0-0.95	0.85	0.84	0.95
ECH	224.60-811.06	811.00	811.00	748.70	0-0.95	0.06	0.06	0.06
MOL	79.99-355.51	356.00	356.00	266.62	0-0.95	0.11	0.12	0.08
POL	49.00-350.00	148.41	163.44	233.33	0-0.95	0.52	0.32	0.28
OBI	65.00-381.33	87.00	89.03	97.50	0-0.95	0.91	0.88	0.31

Table 9., cont.

Group	Consumption (t km <sup>-2</sup> yr <sup>-1</sup> )				Ecotrophic efficiency (dimensionless)			
	Constrained range	A1	A2	Ecopath	Constrained range	A1	A2	Ecopath
LZOO	97.83-1437.44	157.25	161.84	397.04	0-0.95	0.83	0.79	0.95
SZOO	173.60-1131.31	1130.00	1114.83	629.60	0-0.95	0.35	0.40	0.95
PHY					0-0.95	0.66	0.66	0.31
DET <sup>a</sup>					-	1.00	1.00	0.59

<sup>a</sup>: For Detritus, the EE is the ratio between the sum of inputs (egestion and mortality) and the sum of outputs (consumption of detritus).

Table 10. Diet composition (proportion of prey in diet by mass, %) for skates and large crustaceans estimated by inverse modelling. The lower and upper range constraints of diet and the results of the Ecopath model are also presented for comparison. A1: initial inverse model, A2: model with modified weights for diet terms, Ecopath: model of Bundy *et al.* (2000). See Table 1 for group name meanings.

Prey	Skates					Large crustaceans				
	A1	A2	Ecopath	Min	Max	A1	A2	Ecopath	Min	Max
SCO	4.9	4.9	5.0	4.9	6.2					
SGH	0.1	0.1	0.1	0.1	0.2					
SAP	0.1	0.1	0.1	0.1	0.2					
FLO	0.8	0.8	0.7	0.7	0.9					
RED	18.3	9.6	8.6	8.6	21.6					
SDF	14.5	18.7	11.1	11.1	24.0	4.1	4.1	0.0	0.0	5.0
CAP	10.0	9.9	8.0	2.6	10.0					
SLA	17.1	16.7	14.5	14.4	18.2					
ACO	0.1	0.1	0.1	0.1	0.2					
PISF	5.9	6.4	5.8	5.8	7.2					
PLSF	0.8	0.8	0.7	0.7	0.9					
SHR	1.2	1.2	1.5	1.2	2.2	2.0	2.0	2.0	2.0	4.9
LCRU	17.2	20.1	21.6	17.2	31.1			1.0	1.0	11.1
ECH	0.3	0.3	0.3	0.2	0.4	24.3	25.9	30.0	20.0	30.0
MOL	1.2	1.2	1.2	0.8	1.5	17.4	17.8	12.0	12.0	19.8
POL	5.8	7.4	18.6	4.5	8.0	29.1	27.0	30.0	19.6	30.0
OBI	1.0	1.0	1.0	0.7	1.3	3.4	4.7	12.0	0.1	12.0
LZOO	0.3	0.3	1.0	0.2	0.4	4.9	3.9	2.0	2.0	4.9
SZOO	0.1	0.1	0.1	0.0	0.1	4.9	4.9	1.0	1.0	4.9
PHY										
DET						9.8	9.8	10.0	9.7	10.0
Total	100.0	100.0	100.0	74.2	134.6	100.0	100.0	100.0	67.4	132.6



Table 11. Mortality rates ( $t\ km^{-2}\ yr^{-1}$ ) and details of mortality (%) estimated from the inverse A2 and Ecopath models. Z: total mortality ( $Z = Exp + M2 + M0$ ), % Exp: % of mortality by fishing (= export here), %M2: % of mortality by predation, %M0: % of other natural causes of death. See Table 1 for group name meanings.

Group	Z		%Exp		%M2		%M0	
	A2	Ecopath	A2	Ecopath	A2	Ecopath	A2	Ecopath
WHA	0.03	0.03					100%	100%
HAS	0.03	0.02	3%	9%			97%	91%
HOS	0.004	0.004	5%	0%			95%	100%
SEA	0.007	0.003	15%	32%			85%	68%
LCO	1.65	1.35	37%	45%	5%	6%	58%	48%
SCO	0.49	0.44			95%	95%	5%	5%
LGH	0.14	0.10	26%	34%	17%	28%	57%	38%
SGH	0.57	0.41	0%	0%	75%	95%	24%	5%
LAP	0.32	0.52	31%	19%			69%	81%
SAP	0.75	0.49	3%	5%	32%	40%	65%	55%
FLO	0.68	0.40	12%	19%	48%	76%	40%	5%
SKA	0.19	0.07	19%	50%	2%	4%	79%	46%
RED	0.55	0.53	32%	33%	48%	61%	20%	6%
LDF	0.19	0.22	28%	23%	52%	46%	20%	31%
SDF	2.92	0.95			47%	95%	53%	5%
CAP	17.34	15.15	1%	1%	94%	84%	6%	15%
SLA	2.99	2.66			81%	95%	19%	5%
ACO	1.37	1.12			78%	95%	22%	5%
LPF	0.03	0.01	20%	53%	75%	43%	5%	5%
PISF	1.00	0.84	2%	2%	84%	93%	14%	5%
PLSF	2.13	1.62	1%	2%	66%	92%	33%	6%
SHR	1.43	1.18	0%	0%	95%	95%	5%	5%
LCRU	1.08	0.78	1%	2%	83%	93%	16%	4%
ECH	72.99	67.38			6%	7%	94%	93%
MOL	32.04	24.00	0%	0%	12%	9%	88%	91%
POL	22.88	21.00			32%	28%	68%	72%
OBI	12.04	19.50			88%	30%	12%	70%
LZOO	48.55	69.84			79%	95%	21%	5%
SZOO	342.90	255.90			40%	95%	60%	5%
PHY	1790.00	2500.67			66%	31%	34%	69%

Table 12. Distribution of predation mortality (PM expressed by prey biomass,  $\Sigma Pr_X \rightarrow Y/B_X$ , per year; in decreasing order) among vertebrate predators on all prey as estimated from the inverse A2 and Ecopath models. The fishing mortality is also shown for comparison. See Table 1 for group name meanings.

Predator	PM		Rank	
	A2	Ecopath	A2	Ecopath
LCO	3.15	1.35	1	3
HAS	2.80	1.90	2	2
SDF	2.47	0.60	3	8
CAP	2.32	2.53	4	1
Fishing	1.17	1.16	5	4
WHA	1.06	0.87	6	5
PISF	0.73	0.42	7	16
PLSF	0.69	0.55	8	10
HOS	0.63	0.49	9	12
SKA	0.59	0.39	10	18
LGH	0.56	0.44	11	14
RED	0.56	0.53	12	11
SAP	0.52	0.55	13	9
LCRU	0.41	0.62	14	7
SLA	0.41	0.68	15	6
SCO	0.39	0.41	16	17
LDF	0.36	0.42	17	15
LAP	0.31	0.27	18	21
SGH	0.27	0.36	19	19
ACO	0.21	0.34	20	20
FLO	0.18	0.46	21	13
SEA	0.16	0.10	22	23
SHR	0.13	0.16	23	22
LPF	0.04	0.03	24	24

Table 13. Comparisons between key global indices of ecosystem structure for the two mass balance models developed for the Newfoundland–Labrador Shelf for the 1985-1987 period. Here the inv-eco A2 solution is the solution obtained using the outputs from the inverse A2 model as inputs to the Ecopath software (Christensen and Pauly 1992). The total system throughput is the sum of all flows (consumption, exports, respiration, and total flows to detritus) in the system. The connectance index for a given food web is the ratio of the number of actual links to the number of possible links. The system omnivory index is defined as the average omnivory index of all consumers weighted by the logarithm of each consumer's food intake.

Parameters	Ecopath solution	Inv-eco A2 solution	% Difference
Sum of all consumption ( $\text{t km}^{-2} \text{ yr}^{-1}$ )	2518.74	2850.72	13%
Sum of all exports ( $\text{t km}^{-2} \text{ yr}^{-1}$ )	972.27	3.10	-100%
Sum of all respiratory flows ( $\text{t km}^{-2} \text{ yr}^{-1}$ )	1528.40	1786.95	17%
Sum of all flows into detritus ( $\text{t km}^{-2} \text{ yr}^{-1}$ )	2361.74	1449.03	-39%
Total system throughput ( $\text{t km}^{-2} \text{ yr}^{-1}$ )	7381.14	6089.80	-17%
Sum of all production ( $\text{t km}^{-2} \text{ yr}^{-1}$ )	2987.27	2357.33	-21%
Total net primary production ( $\text{t km}^{-2} \text{ yr}^{-1}$ )	2500.67	1790.05	-28%
Total catches ( $\text{t km}^{-2} \text{ yr}^{-1}$ )	1.30	1.30	0%
Total biomass (excluding detritus) ( $\text{t km}^{-2}$ )	287.49	274.80	-4%
Gross efficiency (catch/ $P_{\text{PHY}}$ ) (dimensionless)	0.0005	0.0007	40%
Total primary production/total respiration	1.64	1.00	-39%
Total primary production/total biomass	8.70	6.51	-25%
Total biomass/total throughput	0.04	0.05	15%
Connectance Index	0.29	0.28	-3%
System Omnivory Index	0.13	0.11	-14%
Mean trophic level of fishery	4.83	4.77	-1%

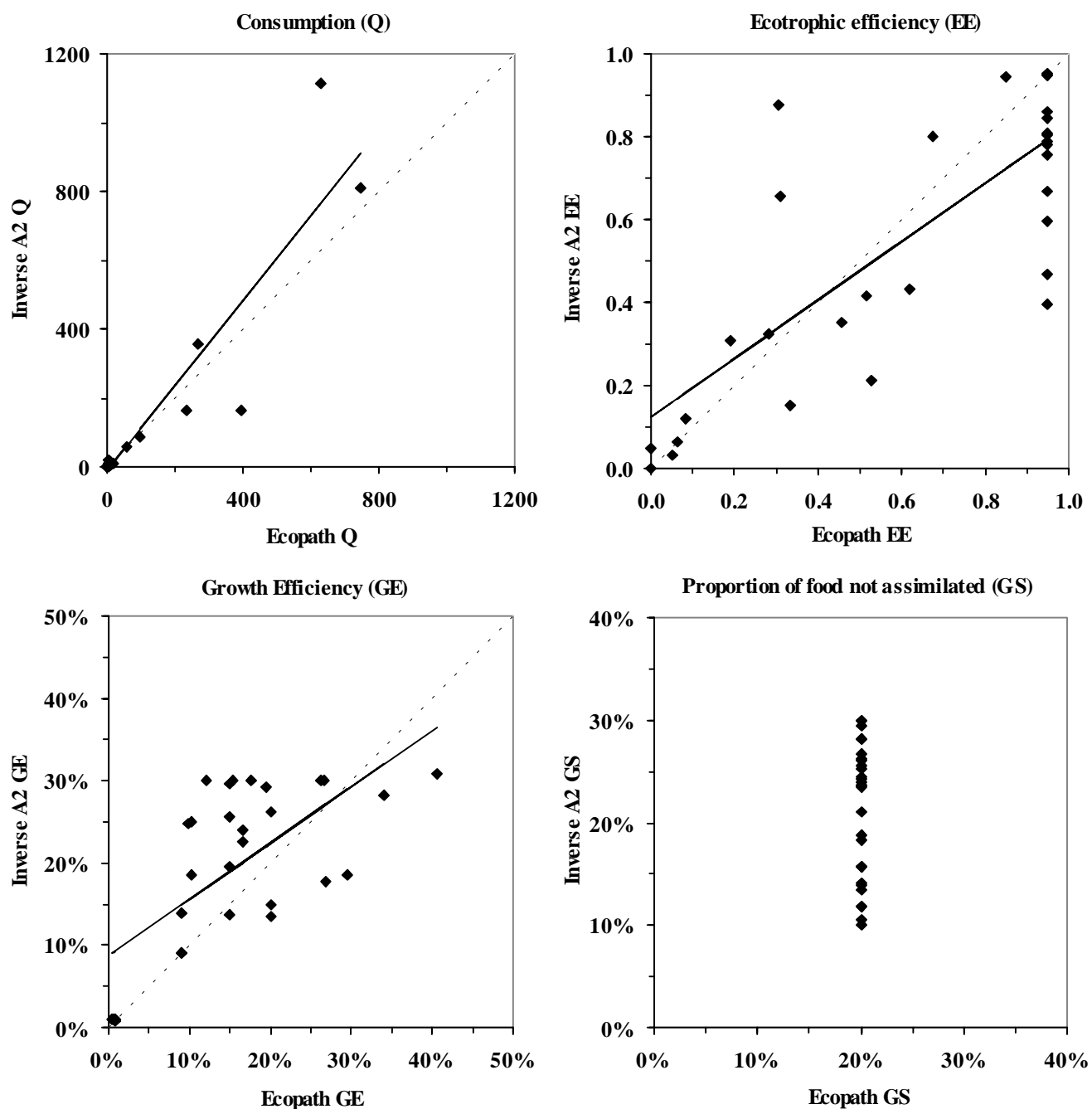


Figure 1. Relationships of consumption ( $Q$  in  $\text{t km}^{-2} \text{yr}^{-1}$ ), growth efficiency ( $GE$  in %), ecotrophic efficiency ( $EE$ , dimensionless), and proportion of unassimilated food ( $GS$  in %) between the inverse A2 and Ecopath models. If applicable, the line 1:1 (dotted line) and the regression line (solid line) are also shown for comparison.

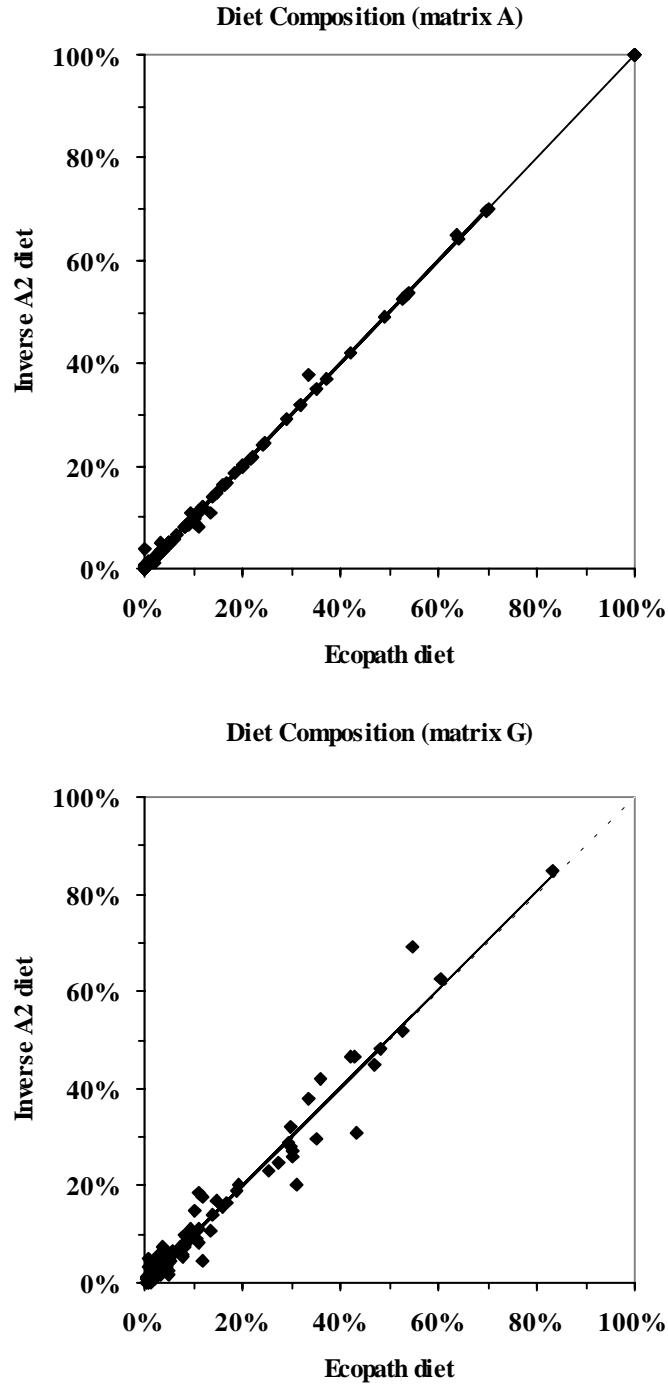


Figure 2. Relationships of diet composition for values with modified weights (matrix A) and for constrained values (matrix G) between the inverse A2 and Ecopath models. The line 1:1 is also shown for comparison.

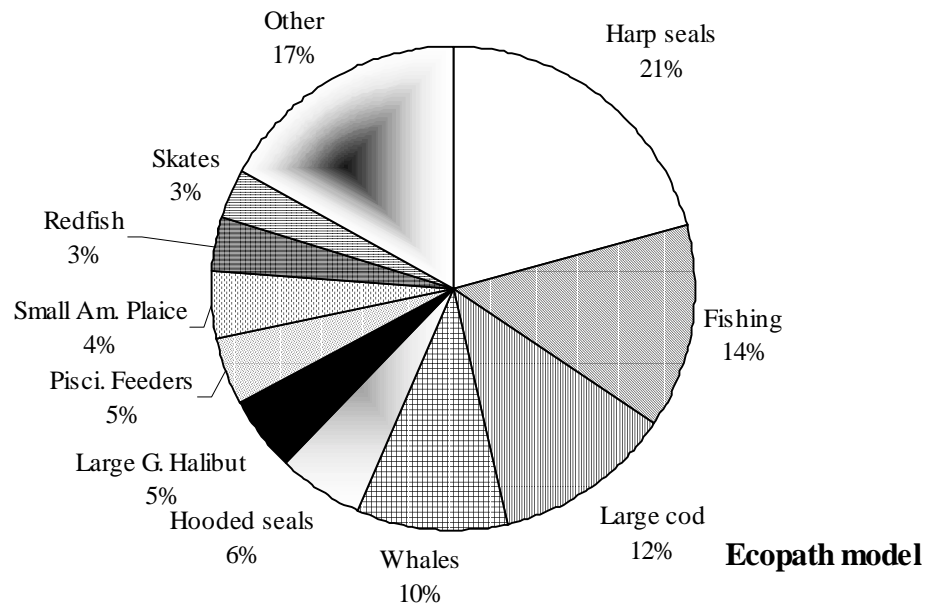
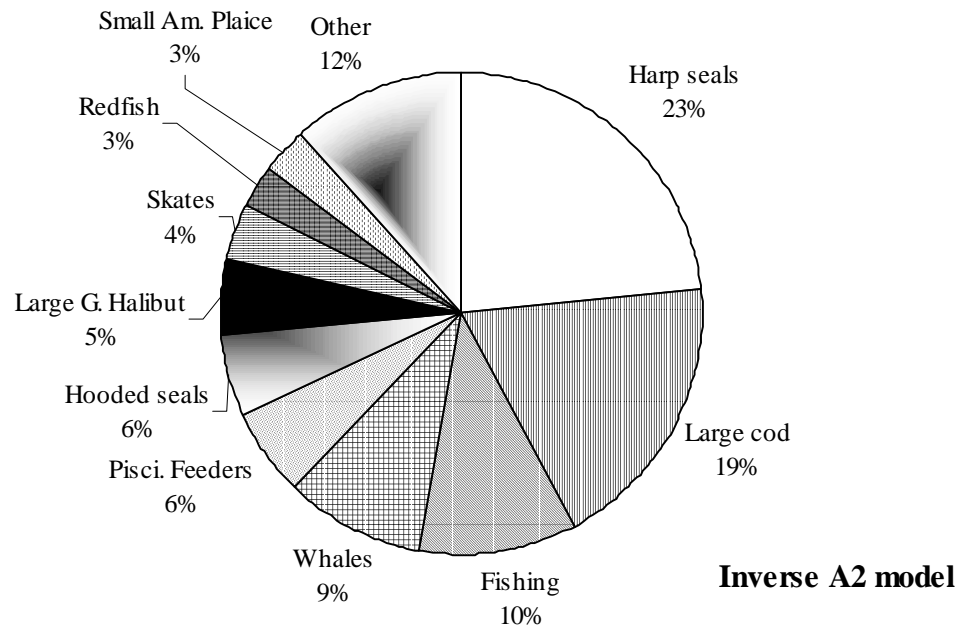


Figure 3. Distribution of predation mortality (expressed by prey biomass,  $\Sigma Pr_X \rightarrow Y/B_X$ ) on fish prey for the inverse A2 and Ecopath models. Fishing is also shown for comparison.

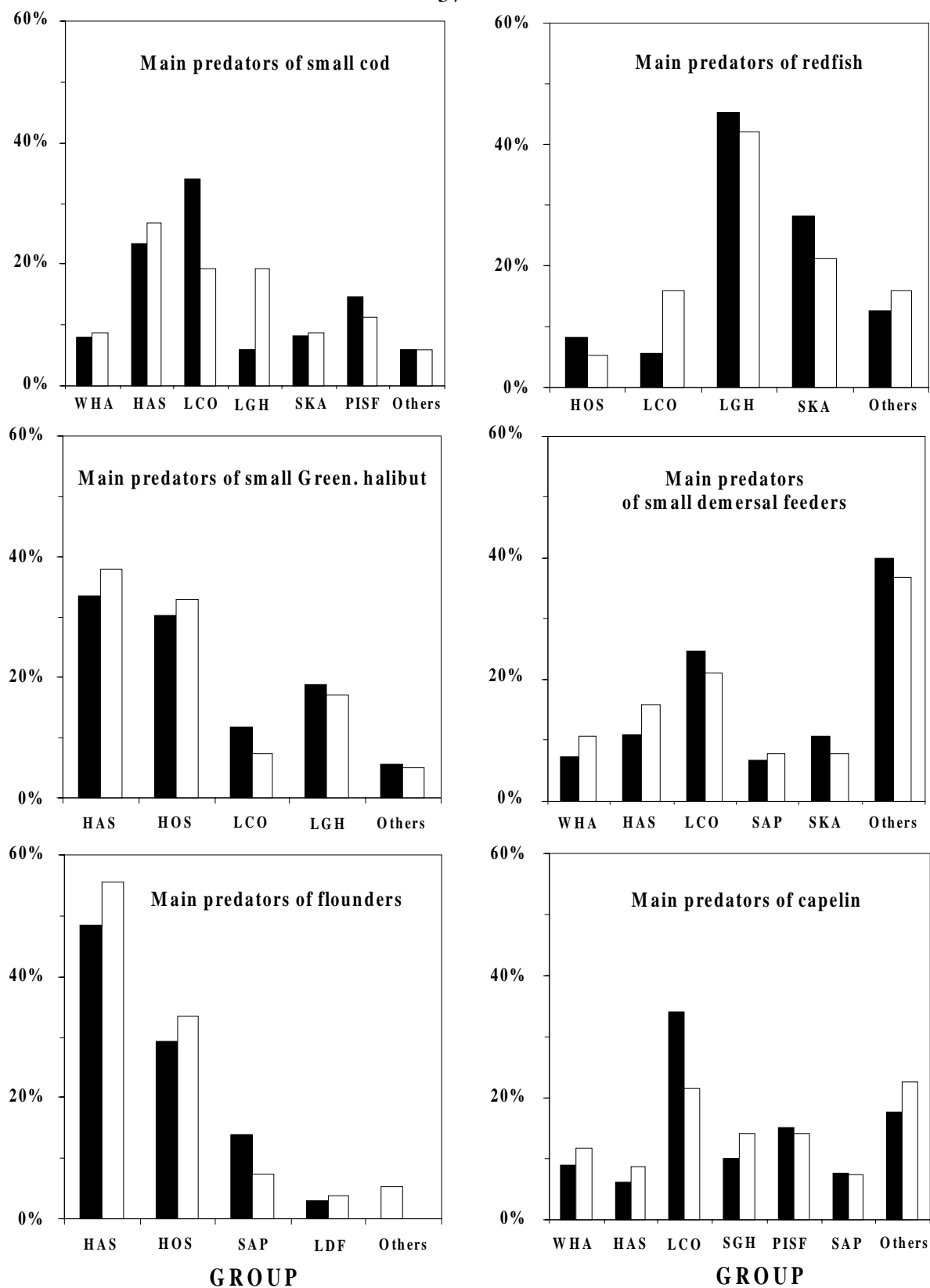


Figure 4. Composition of main predators on small cod ( $\leq 35$  cm), small Greenland halibut ( $\leq 40$  cm), flounders, redfish, small demersal feeders, and capelin for the inverse A2 (black bars) and Ecopath (white bars) models.

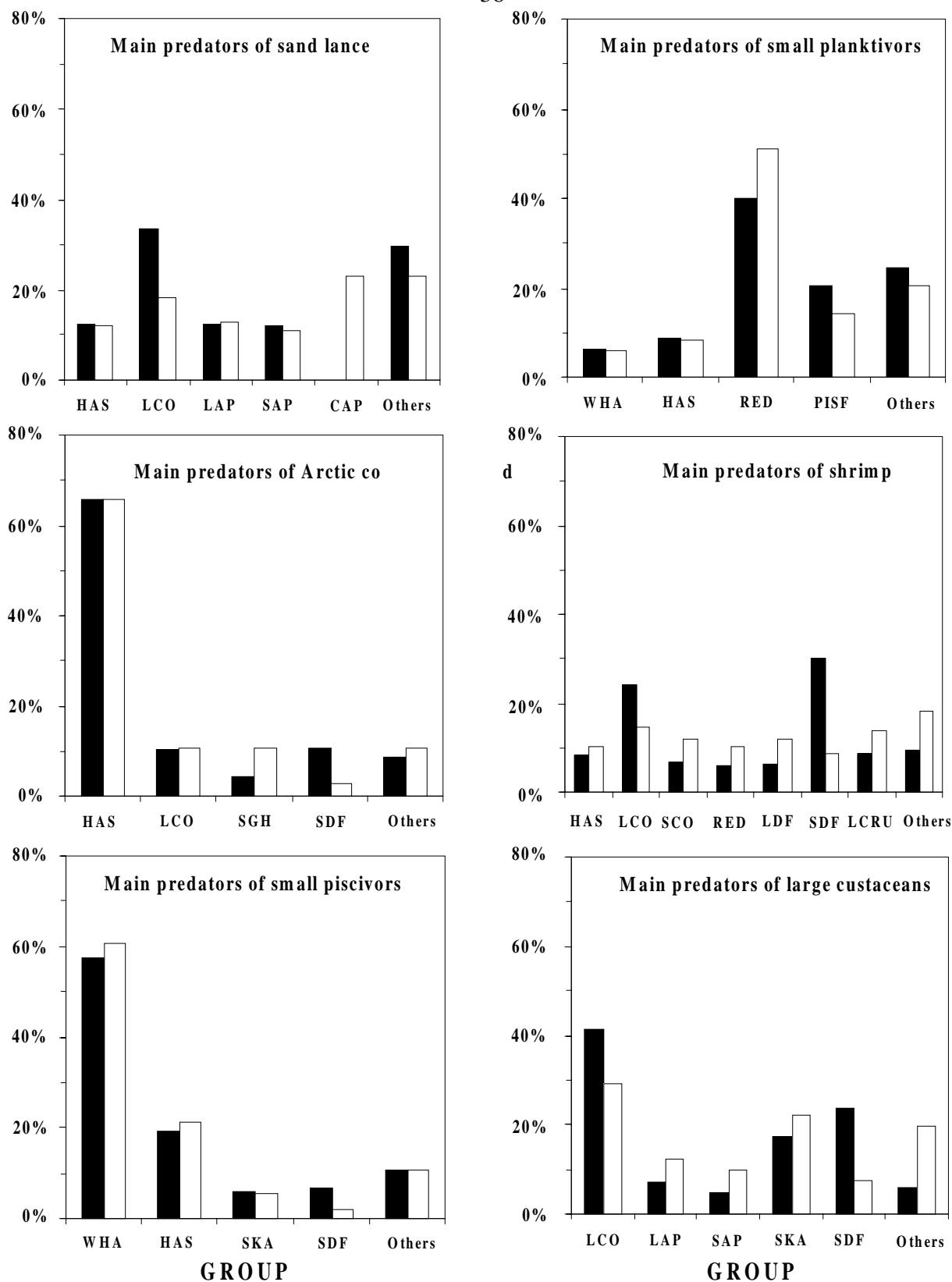


Figure 5. Composition of main predators on sand lance, Arctic cod, piscivorous small pelagic feeders, planktivorous small pelagic feeders, shrimp, and large crustaceans for the inverse A2 (black bars) and Ecopath (white bars) models.



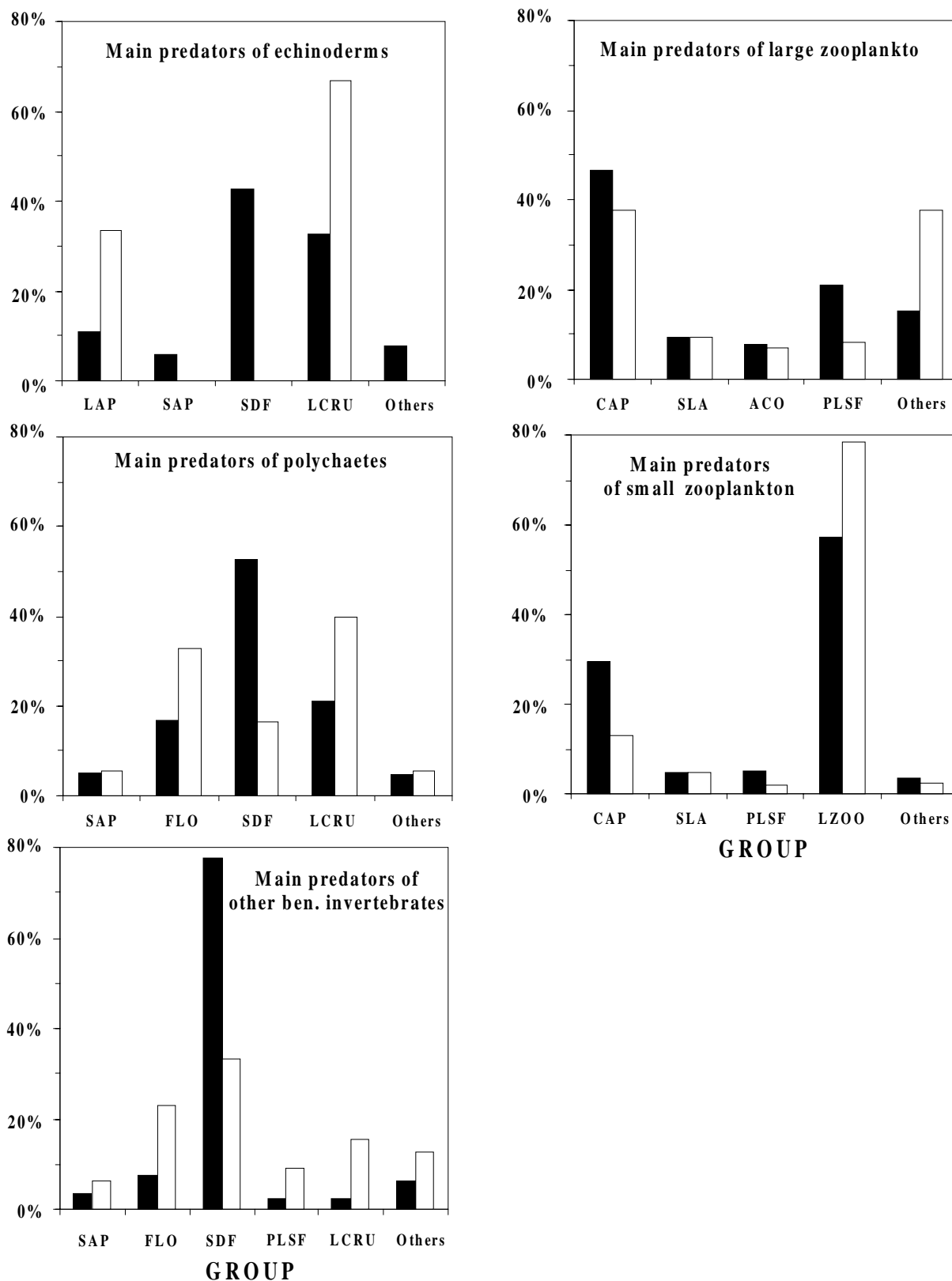


Figure 6. Composition of main predators on echinoderms, polychaetes, other benthic invertebrates, large zooplankton (> 5 mm), and small zooplankton (< 5 mm) for the inverse A2 (black bars) and Ecopath (white bars) models.

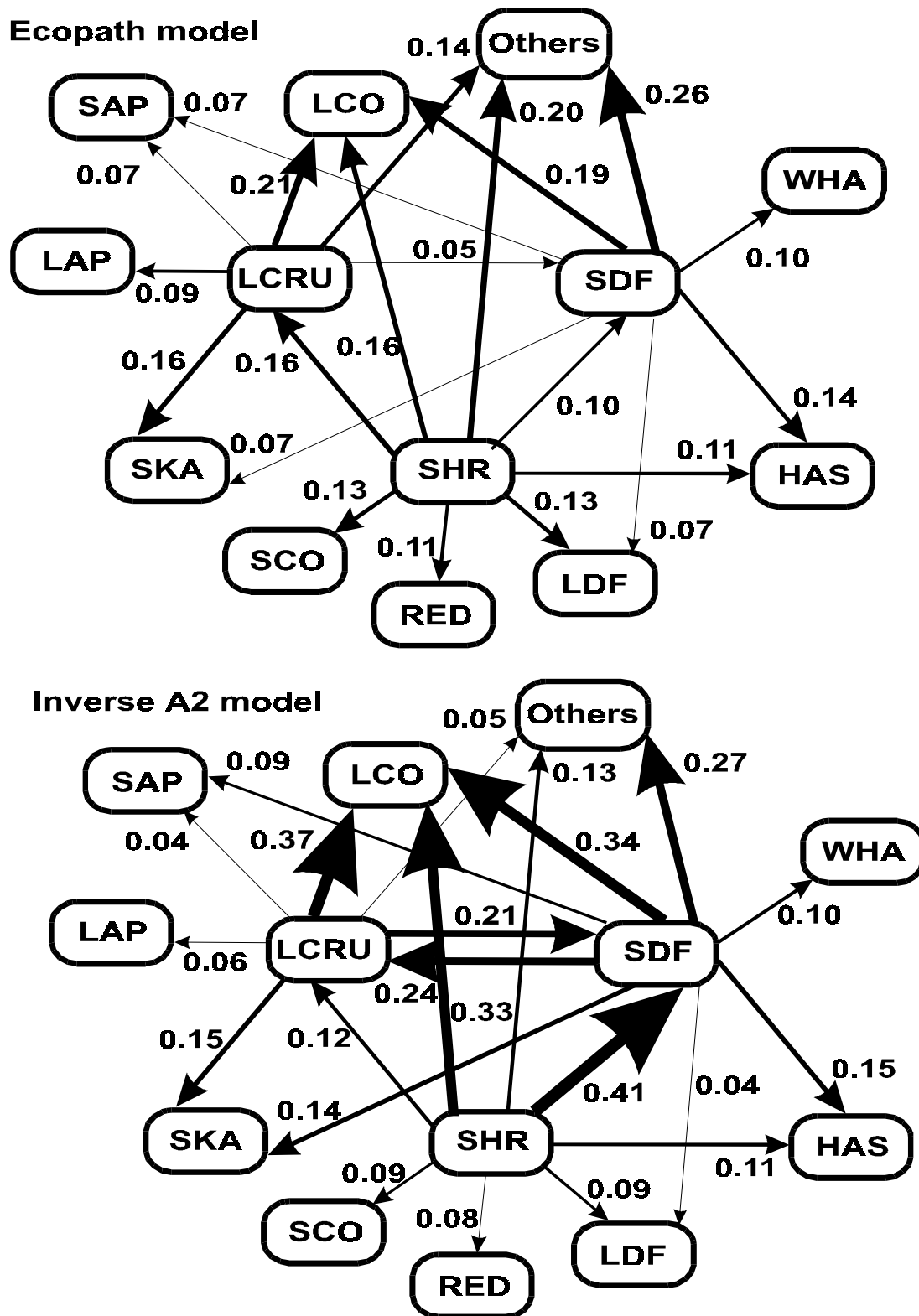


Figure 7. Composition of predation mortality (flux in  $\text{t km}^{-2} \text{ yr}^{-1}$ ) on small demersal feeders (SDF), large crustacea (LCRU), and shrimp (SHR) for the Ecopath and inverse A2 models. See Table 1 for group name meanings.

Appendix 1. Diet matrix for inverse modelling. TRN: number of trophic relations; SD: standard deviation. The diets with SD greater than 0.6% (in bold) were used as constraints in matrix G. All values are percentages except TRN.

Prey	Predator											
	WHA	HAS	HOS	SEA	LCO				SCO			
					Mean	± SD	Min	Max	Mean	± SD	Min	Max
LCO		1.3	9.3									
SCO	1.2	3.4		0.5	1.8	0.3	1.4	2.1	0.7	<b>0.7</b>	0.0	1.3
LGH		0.4	3.6									
SGH		4.5	29.0		0.6	0.3	0.3	0.8	0.2	0.3	0.0	0.5
LAP												
SAP		1.0			1.7	<b>0.6</b>	1.2	2.3	0.0	0.1	0.0	0.1
FLO		5.0	21.6		0.1	0.1	0.0	0.2	0.0	0.0	0.0	0.0
SKA					0.0	0.0	0.0	0.1				
RED		0.5	4.9		0.9	<b>1.0</b>	0.0	1.8	0.0	0.1	0.0	0.1
LDF	3.3											
SDF	3.3	4.7	12.0	1.6	4.0	<b>0.9</b>	3.1	4.9	2.4	<b>1.4</b>	1.0	3.8
CAP	48.9	31.9	0.8	70.0	60.3	<b>2.4</b>	57.9	62.7	43.0	<b>3.5</b>	39.5	46.4
SLA	5.2	9.5		5.0	10.5	<b>1.9</b>	8.6	12.3	3.1	<b>2.4</b>	0.7	5.5
ACO		21.9	1.4	6.0	2.2	<b>0.9</b>	1.2	3.1	3.2	<b>1.5</b>	1.7	4.7
LPF		0.1		0.1								
PISF	16.3	5.1	2.8	1.6	0.1	0.0	0.1	0.2	0.5	0.0	0.4	0.5
PLSF	3.0	3.8	14.7	2.9	0.4	0.1	0.3	0.5	1.4	0.1	1.2	1.5
SHR		3.6		0.6	3.7	0.2	3.5	3.9	7.9	<b>2.7</b>	5.2	10.5
LCRU					4.8	<b>0.7</b>	4.2	5.5	2.2	<b>0.6</b>	1.6	2.9
ECH					0.4	0.1	0.4	0.5	0.0	0.0	0.0	0.0
MOL				0.1	2.3	0.5	1.8	2.8	0.6	<b>0.6</b>	0.1	1.2
POL					0.6	0.2	0.4	0.8	1.7	0.5	1.2	2.2
OBI		0.3			1.0	0.1	0.9	1.2	13.9	<b>1.1</b>	12.8	15.0
LZOO	10.4	2.9		11.1	4.7	<b>2.0</b>	2.7	6.7	19.3	<b>2.7</b>	16.6	21.9
SZOO	8.3			0.5	0.0	0.0	0.0	0.0	0.0	0.0	0.0	0.0
PHY												
DET												
Total	100.0	100.0	100.0	100.0	100.0		87.8	112.3	100.0		81.9	118.3
TRN	9	17	10	12	20		20	20	19		19	19

## Appendix 1., cont.

Prey	Predator											
	LGH				SGH				LAP			
	Mean	± SD	Min	Max	Mean	± SD	Min	Max	Mean	± SD	Min	Max
LCO												
SCO	7.9	<b>2.6</b>	5.3	10.5	0.9	<b>0.8</b>	0.1	1.6	0.0	0.0	0.0	0.0
LGH												
SGH	16.0	<b>9.3</b>	6.7	25.3	0.5	0.5	0.0	1.1	0.5	<b>0.7</b>	0.0	1.2
LAP												
SAP	0.5	<b>0.8</b>	0.0	1.3					0.1	0.0	0.1	0.1
FLO	0.2	0.2	0.0	0.4					0.0	0.0	0.0	0.0
SKA	0.1	0.2	0.0	0.3								
RED	25.4	<b>7.7</b>	17.7	33.2	0.0	0.0	0.0	0.0				
LDF												
SDF	7.9	<b>2.0</b>	5.9	10.0	0.8	<b>0.7</b>	0.1	1.4	0.9	0.5	0.5	1.4
CAP	36.1	<b>7.5</b>	28.6	43.5	83.4	<b>1.5</b>	81.9	84.9	29.6	<b>3.5</b>	26.1	33.1
SLA					0.0	0.0	0.0	0.1	16.8	<b>0.9</b>	15.9	17.7
ACO	1.9	<b>1.4</b>	0.5	3.3	5.0	<b>3.0</b>	2.0	8.0	0.1	0.0	0.1	0.1
LPF	0.2	0.2	0.0	0.5								
PISF	0.5	0.2	0.4	0.7	1.0	0.2	0.8	1.2	0.0	0.0	0.0	0.0
PLSF	1.6	0.5	1.1	2.0	3.0	<b>0.7</b>	2.3	3.7	0.0	0.0	0.0	0.1
SHR	1.1	0.1	1.1	1.2	2.2	0.6	1.6	2.8	0.3	0.0	0.3	0.3
LCRU	0.1	0.1	0.0	0.2					4.4	<b>2.1</b>	2.3	6.6
ECH					0.0	0.0	0.0	0.0	29.6	<b>3.2</b>	26.5	32.8
MOL	0.0	0.1	0.0	0.1					8.0	<b>1.8</b>	6.3	9.8
POL	0.0	0.0	0.0	0.0	0.0	0.0	0.0	0.0	1.6	<b>1.2</b>	0.5	2.8
OBI	0.1	0.1	0.0	0.2	0.3	0.2	0.1	0.6	5.8	<b>2.6</b>	3.2	8.4
LZOO	0.2	0.1	0.1	0.4	2.9	<b>3.1</b>	0.0	6.0	2.0	0.5	1.6	2.5
SZOO	0.0	0.0	0.0	0.0	0.0	0.0	0.0	0.0	0.0	0.0	0.0	0.0
PHY												
DET												
Total	100.0		67.3	133.0	100.0		88.9	111.3	100.0		83.2	117.0
TRN	19		19	19	15		15	15	18		18	18

## Appendix 1., cont.

Prey	Predator											
	SAP				FLO				SKA			
	Mean	± SD	Min	Max	Mean	± SD	Min	Max	Mean	± SD	Min	Max
LCO												
SCO	0.4	<b>0.6</b>	0.0	1.0					<b>5.3</b>	<b>0.9</b>	4.9	6.2
LGH												
SGH	0.2	0.0	0.2	0.2					<b>0.1</b>	0.0	0.1	0.2
LAP												
SAP	2.1	<b>2.5</b>	0.0	4.6					<b>0.1</b>	0.0	0.1	0.2
FLO	0.8	<b>1.1</b>	0.0	1.9					<b>0.8</b>	0.1	0.7	0.9
SKA												
RED	0.1	0.0	0.1	0.1					<b>14.5</b>	<b>9.1</b>	8.6	21.6
LDF												
SDF	2.3	<b>1.6</b>	0.7	3.9	0.7	<b>3.9</b>	0.0	4.6	<b>16.8</b>	<b>9.1</b>	11.1	24.0
CAP	33.3	<b>4.3</b>	29.0	37.7	2.5	<b>2.3</b>	0.2	4.7	<b>6.0</b>	<b>5.3</b>	2.6	10.0
SLA	9.0	<b>2.9</b>	6.1	12.0	2.5	<b>2.3</b>	0.2	4.9	<b>15.6</b>	<b>2.6</b>	14.4	18.2
ACO	0.4	0.0	0.4	0.4					<b>0.1</b>	0.0	0.1	0.2
LPF												
PISF	0.0	0.0	0.0	0.0					<b>6.2</b>	<b>1.0</b>	5.8	7.2
PLSF	0.0	0.0	0.0	0.0					<b>0.8</b>	0.1	0.7	0.9
SHR	1.3	0.0	1.3	1.3	0.7	<b>1.2</b>	0.0	1.9	<b>1.6</b>	<b>0.7</b>	1.2	2.2
LCRU	2.1	<b>1.4</b>	0.7	3.5	0.0	0.1	0.0	0.1	<b>23.1</b>	<b>9.8</b>	17.2	31.1
ECH	11.2	<b>4.2</b>	7.0	15.4	5.3	<b>5.0</b>	0.4	10.3	<b>0.3</b>	0.1	0.2	0.4
MOL	3.1	<b>2.4</b>	0.7	5.5	3.5	<b>7.0</b>	0.0	10.5	<b>1.1</b>	0.5	0.8	1.5
POL	11.1	<b>2.2</b>	8.9	13.2	47.0	<b>26.4</b>	20.6	73.4	<b>6.0</b>	<b>2.5</b>	4.5	8.0
OBI	13.4	<b>6.0</b>	7.4	19.4	35.1	<b>13.6</b>	21.5	48.7	<b>1.0</b>	0.4	0.7	1.3
LZOO	9.2	<b>6.1</b>	3.2	15.3	2.7	<b>2.4</b>	0.3	5.1	<b>0.3</b>	0.1	0.2	0.4
SZOO	0.0	0.0	0.0	0.0					<b>0.1</b>	0.1	0.0	0.1
PHY												
DET												
Total	100.0		65.6	135.3	100.0		43.1	164.2	100.0		74.2	134.6
TRN	19		19	19	10		10	10	19		19	19

## Appendix 1., cont.

Prey	Predator										SLA	ACO
	RED				LDF	SDF	CAP					
	Mean	± SD	Min	Max			Mean	± SD	Min	Max		
LCO												
SCO	0.5	0.4	0.2	0.7	1.1							
LGH												
SGH					0.0							
LAP												
SAP					1.7							
FLO					1.1							
SKA					0.1							
RED	0.7		0.6	0.8	1.6							
LDF												
SDF	0.1	0.1	0.0	0.1	4.2	1.0						
CAP	0.7		0.6	0.8	3.9	2.0	1.0	<b>1.4</b>	0.0	2.5		3.8
SLA	0.2	0.3	0.0	0.4	2.7	1.0	1.0	<b>1.4</b>	0.0	2.5		
ACO						0.5						0.2
LPF												
PISF					0.1	0.2						
PLSF	24.5		22.1	27.0	3.4	0.3						
SHR	3.5		3.2	3.9	9.0	2.0						
LCRU					2.6	1.0						
ECH					19.9	10.0						
MOL					6.7	10.0						
POL					8.0	20.0						
OBI					14.1	42.0						
LZOO	53.8		48.4	59.2	18.5	5.0	43.4	<b>12.5</b>	30.9	55.9	35.0	64.0
SZOO	16.1		14.5	17.7	1.4	5.0	54.6	<b>15.4</b>	39.2	70.0	65.0	32.0
PHY												
DET												
Total	100.0		89.6	110.4	100.0	100.0	100.0		70.1	130.8	100.0	100.0
TRN	9		9	9	19	14	4		4	4	2	4

## Appendix 1., cont.

Prey	Predator													
	LPF				PISF	PLSF				SHR	LCRU			
	Mean	± SD	Min	Max		Mean	± SD	Min	Max		Mean	± SD	Min	Max
LCO														
SCO	0.2	0.2	0.0	0.4	1.9									
LGH														
SGH														
LAP														
SAP														
FLO														
SKA														
RED	0.2	0.2	0.0	0.4										
LDF														
SDF	3.5	<b>4.9</b>	0.0	8.4	0.0						2.5	<b>3.5</b>	0.0	5.0
CAP	7.5	<b>3.5</b>	4.0	11.0	69.8									
SLA	8.6	<b>5.1</b>	3.5	13.7	1.1									
ACO					0.0									
LPF														
PISF	27.3	<b>9.5</b>	17.8	36.8										
PLSF	18.8	<b>2.5</b>	16.3	21.2	8.3									
SHR	1.2	<b>1.2</b>	0.0	2.4	0.8	0.5	<b>0.7</b>	0.0	1.2		3.5	<b>2.1</b>	2.0	4.9
LCRU											6.1	<b>7.1</b>	1.0	11.1
ECH											25.0	<b>7.1</b>	20.0	30.0
MOL											15.9	<b>5.5</b>	12.0	19.8
POL	0.3	0.4	0.0	0.6						1.5	24.8	<b>7.4</b>	19.6	30.0
OBI	1.9	<b>2.3</b>	0.0	4.2		5.0	<b>7.1</b>	0.0	12.1	1.5	6.1	<b>8.4</b>	0.1	12.0
LZOO	29.5	<b>3.0</b>	26.5	32.5	16.8	52.7	<b>1.9</b>	50.7	54.6	12.0	3.5	<b>2.1</b>	2.0	4.9
SZOO	1.3	<b>0.8</b>	0.5	2.0	1.3	41.9	<b>4.5</b>	37.4	46.3	24.0	3.0	<b>2.8</b>	1.0	4.9
PHY										8.5				
DET										52.5	9.9	0.2	9.7	10.0
Total	100.0		68.6	133.5	100.0	100.0		88.1	114.1	100.0	100.0		66.4	121.5
TRN	12		12	12	9	4		4	4	6	10		10	10

## Appendix 1., cont.

Prey	Predator								
	ECH	MOL	POL	OBI	LZOO				SZOO
					Mean	$\pm$ SD	Min	Max	
LCO									
SCO									
LGH									
SGH									
LAP									
SAP									
FLO									
SKA									
RED									
LDF									
SDF									
CAP									
SLA									
ACO									
LPF									
PISF									
PLSF									
SHR									
LCRU									
ECH									
MOL									
POL									
OBI									
LZOO					5.0				
SZOO					43.0	<b>7.1</b>	38.0	48.0	
PHY					37.0				100.0
DET	100.0	100.0	100.0	100.0	15.0	<b>7.1</b>	10.0	20.0	
Total	100.0	100.0	100.0	100.0	100.0		48.0	68.0	100.0
TRN	1	1	1	1	4		2	2	1



## Appendix 2. A simple three-compartment example of the inverse solution process.

The approach can be illustrated with a simple example (Fig. A). Consider a food web made up of just three compartments: a primary producer (P), a consumer (Z), and a detritus pool (D). Assume that we know the flows entering and leaving this food web and exchanging among the pools and that these flows are in steady state. In this case, the flows are known because they are the product of a computer simulation (Franck Touratier, Laval Univ., Qc, pers. comm.). The problem is to calculate all the flows when we know only a fraction of them.

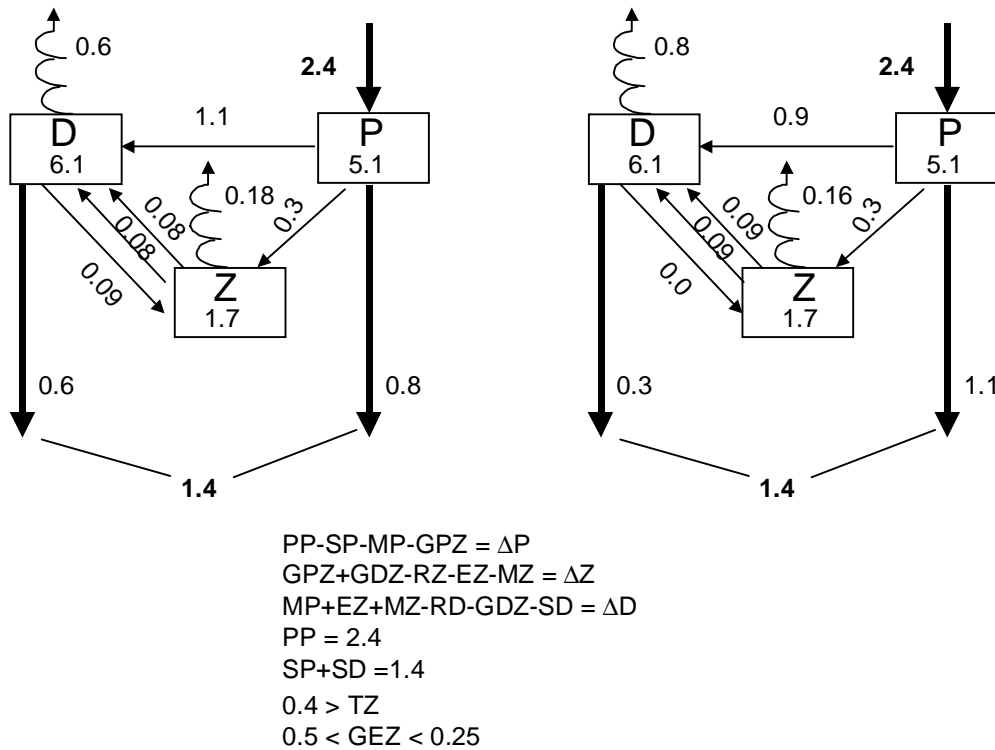


Figure A. A simple example of an inverse analysis. The diagram on the left represents the inter-compartmental flows and the biomasses resulting from a one-month simulation using a three-compartment model. The diagram on the right is a reconstruction of the flows using only the primary production and sedimentation flows as input data. PP: primary production, SP: sedimentation of phytoplankton, MP: mortality of phytoplankton, GPZ: grazing of phytoplankton by the zooplankton, GDZ: grazing of detritus by zooplankton, RZ: respiration of zooplankton, EZ: egestion by zooplankton, MZ: mortality of zooplankton, RD: remineralization of detritus, SD: sedimentation of detritus, GEZ: growth efficiency of zooplankton, and TZ: turnover rate of zooplankton. Here, it was assumed that there was no year-to-year change in standing stock (i.e., the food web is in steady state and  $\Delta P$ ,  $\Delta Z$ , and  $\Delta D$  are thus equal to 0).

We can write the mass balance for each of these pools as a sum of inputs and outputs adding up to zero. This gives us three equations with ten variables representing the flows. Assume further that we have independent measurements of primary production (PP) and of sedimentation (S). That gives us two additional equations to yield five equations to solve for the ten flows.

It is possible to solve this system for the ten flows, but it would be better to augment this with other conditions that reflect our prior knowledge of this system. First, we specify that all the flows must be nonnegative since the direction of the flow is provided for in the equations. We specify further that the efficiency with which Z transforms its consumption into biomass falls between 0.25 and 0.50 and that this compartment turns over no faster than  $0.4 \text{ d}^{-1}$ . These inequality relations are appended to the equality relations to form a system of  $y$  equations to be solved for the ten flows.

Figure A shows the solution for the flows calculated from this system of equations. This is the solution that minimizes errors between the assumed and calculated mass balances and between the measured and calculated PP and S. It is also the solution that minimizes the sum of the flows through the food web.

We have not recovered the original flows exactly; however, the correlation between the known flows and their inverse estimates is 0.97 and the slope and intercepts of the predicted/observed relationship indicate no bias (intercept is zero and the slope is one). With this very simple system, the inverse recalculation works well. Of course, as we increase the complexity of the ecosystem to model, the reconstruction becomes less reliable and we need to be more cautious in the interpretation of the results.

## MASS BALANCE EQUATIONS

### Writing the equations in matrix form

The first step is to write out the equations in matrix form (Fig. B) and set up a rectangular matrix to represent the connections in the food web. The rows of the matrix are the mass balance relations; there are as many rows as there are equations. The columns of the matrix are the flows; there are as many columns as there are flows in the food web. In this simple case, the entries in the matrix are either zero, 1, or  $-1$ . A zero indicates that there is no relationship between the flow in column  $j$  and the relation in row  $i$ . It is the most frequent case (i.e., matrix is sparse).

A value of 1 indicates that the flow in column  $j$  is an input to the mass balance or relation represented in row  $i$ . So, in the case of flow PP, it is an input for the P compartment (row 1) and an input also in the relation that specifies the measured primary production (row 4). Conversely, a value of  $-1$  indicates that the flow in column  $j$  is an output from compartment  $i$  or from a relation that specifies a measured flow. In the case of flow SD, it is an output from the D compartment (row 3) but also an input in calculating total sedimentation (row 5).

$$\begin{aligned}
&PP-SP-MP-GPZ = \Delta P \\
&GPZ+GDZ-RZ-EZ-MZ = \Delta Z \\
&MP+EZ+MZ-RD-GDZ-SD = \Delta D \\
&PP = 2.4 \\
&SP+SD = 1.4
\end{aligned}$$

<b>A</b>	PP	GPZ	MP	RZ	EZ	MZ	GDZ	RD	SD	SP		<b>b</b>
P	1	-1	-1	0	0	0	0	0	0	-1	=	0.0
Z	0	1	0	-1	-1	-1	1	0	0	0	=	0.0
D	0	0	1	0	1	1	-1	-1	-1	0	=	0.0
PP	1	0	0	0	0	0	0	0	0	0	=	2.4
S	0	0	0	0	0	0	0	0	1	1	=	1.4

$$\begin{aligned}
&\text{Minimize} && \| \mathbf{Ax} - \mathbf{b} \| \\
&\text{and} && \| \mathbf{x} \| \\
&\text{subject to} && \mathbf{Ax} = \mathbf{b} + \varepsilon
\end{aligned}$$

Figure B. Setting up the mass balance relations as a matrix algebra problem. Here, it was assumed that there was no year-to-year change in standing stock (i.e., the food web is in steady state and  $\Delta P$ ,  $\Delta Z$ , and  $\Delta D$  are thus equal to 0).

Once the matrix  $\mathbf{A}$  is constructed, we specify a vector  $\mathbf{b}$  that has as many rows as  $\mathbf{A}$  and that gives the expected values of the mass balance relations (zero in the steady state case; rows 1-3) and the values of the measured flows (PP and S; rows 4-5). What we want to calculate then is a vector  $\mathbf{x}$  that has as many elements as there are columns in  $\mathbf{A}$  and that represents the flows that once multiplied by  $\mathbf{A}$  approximate the vector  $\mathbf{b}$ . In short, we want to solve the system  $\mathbf{Ax} = \mathbf{b}$  for the  $\mathbf{x}$  that minimizes  $\|\mathbf{Ax}-\mathbf{b}\|$  (i.e., the sum of squared deviations) and  $\|\mathbf{x}\|$  (i.e., the sum of squared flows).

## CONSTRAINT EQUATIONS

Writing the equations in matrix form

The inequality relations can also be written in matrix form (Fig. C) by setting up a matrix with as many rows as there are inequality relations and with the same number of columns (representing the flows) as  $\mathbf{A}$ . As for  $\mathbf{A}$ , most of the entries are zero. Non-zero entries are to specify a constraint  $i$  on flow  $j$ . For a constraint of non-negativity for flow  $j$ , we initially enter 1 under column  $j$ . However, the quadratic programming procedure (below) is set up to solve less

than or equal inequalities ( $\leq$ ) only. To implement a greater than or equal inequality ( $\geq$ ), we simply multiply the whole row through by  $-1$ . So, the entry under column  $j$  for this constraint is  $-1$ .

G	PP	GPZ	MP	RZ	EZ	MZ	GDZ	RD	SD	SP			h	
PP	-1	0	0	0	0	0	0	0	0	0	<		0	
GPZ	0	-1	0	0	0	0	0	0	0	0	<		0	
MP	0	0	-1	0	0	0	0	0	0	0	<		0	
RZ	0	0	0	-1	0	0	0	0	0	0	<		0	
EZ	0	0	0	0	-1	0	0	0	0	0	<		0	
MZ	0	0	0	0	0	-1	0	0	0	0	<		0	
GDZ	0	0	0	0	0	0	-1	0	0	0	<		0	
RD	0	0	0	0	0	0	0	-1	0	0	<		0	
SD	0	0	0	0	0	0	0	0	-1	0	<		0	
SP	0	0	0	0	0	0	0	0	0	-1	<		0	
<div>Gx ≤ h</div>														
		G	PP	GPZ	MP	RZ	EZ	MZ	GDZ	RD	SD	SP		h
RZ+EZ-0.75*(GPZ+GDZ)>0			0.00	-0.75	0.00	1.00	1.00	0.00	-0.75	0.00	0.00	0.00	<	0
RZ+EZ-0.5*(GPZ+GDZ)>0			0.00	0.50	0.00	-1.00	-1.00	0.00	0.50	0.00	0.00	0.00	<	0
GPZ+GDZ<Z*MaxSpecIng			0	1	0	0	0	0	1	0	0	0	<	0.698

Figure C. Setting up the constraint equations (upper panel). Matrix-vector representation of conversion efficiency and maximum ingestion rate constraints (lower panel).

We can implement more complex constraints in this way. The other constraint we wish to add is that the conversion efficiency falls between 25% and 50%. To implement this requires two inequality relations on the same flows: one to specify the lower bound at 25% and the other to specify the upper bound at 50%. First, we write out the constraint equation for conversion efficiency ( $\Delta B < e \times \Sigma G_j$ ) and using the fact that  $\Delta B = \Sigma G_j - (R+E)$ , we get  $\Sigma G_j - (R+E) < e \times \Sigma G_j$ . Rearranging to collect the  $\Sigma G_j$  terms, we obtain  $(1-e) \times \Sigma G_j - R - E < 0$ . For a lower bound on  $e$  (upper bound on  $(1-e)$ ), we initially specify  $1-e_{low}$  for the columns corresponding to the grazing flows and  $-1$  for the columns corresponding to  $R$  and  $E$ . Remembering that this is actually an upper bound, we multiply everything through by  $-1$ . We do the same thing for the upper bound on  $e$  (lower bound on  $(1-e)$ ), substituting  $e_{high}$  for  $e_{low}$  and keeping the signs as they are.

We implement the constraint on maximum ingestion rate in a similar way, except that now we have an inequality of the form  $\Sigma G_j < y$ , where  $y$  is a constant. We substitute a 1 for each column corresponding to a grazing flow and leave  $y$  on the right-hand side.

We end up with a matrix  $\mathbf{G}$  and a vector  $\mathbf{h}$ , with as many elements as there are rows in  $\mathbf{G}$ , defining the system  $\mathbf{G}\mathbf{x} = \mathbf{h}$ .

## SOLVING THE EQUATIONS

In this case,  $m$ , the number of equations, is less than  $n$ , the number of flows, and we have an underdetermined or rank-deficient system of equations. We can still find a solution if we reduce the dimensionality of the problem from  $n$  (we do not have information for all  $n$ ) to  $m$  (we do have information for all  $m$ ).

How to reduce the dimensionality of the problem? An analogous problem is found in multivariate analyses such as Empirical Orthogonal Functions (EOF) or Principal Components Analysis (PCA), which are more familiar to physicists and biologists respectively. In these very common analyses, we try to reduce a complex multi-dimensional set of observations into a representation in one to three dimensions that represent a substantial portion of the structure in the original data. In our case, we use a decomposition in orthogonal functions or principal components to reduce the dimensionality from  $n$  to  $m$  (it can also be less than  $m$  as we will see later). Once the problem is reduced to  $m$  dimensions, we have the equivalent of a square system of equations and we can solve for a value for  $\mathbf{x}$ .

The reduction in dimensionality is achieved through a mathematical process called Singular Value Decomposition (SVD). The SVD decomposes the matrix  $\mathbf{A}$  into orthogonal vectors  $\mathbf{U}$  and  $\mathbf{V}$  linked by a scale factor ( $\lambda$ ). The vectors  $\mathbf{U}$  and  $\mathbf{V}$  are arranged in decreasing order of  $\lambda$ . The interpretation is that the first pair of  $\mathbf{U}$  and  $\mathbf{V}$  vectors ( $\mathbf{u}_1$  and  $\mathbf{v}_1$ ) are the orthogonal functions that explain the largest proportion of the structure in  $\mathbf{A}$  (measured by  $\lambda_1$ ). So, the product  $\mathbf{u}_1 \times \lambda_1 \times \mathbf{v}_1'$  gives a first approximation to  $\mathbf{A}$  ( $\mathbf{A}_1$ ). If we add the second pair of vectors ( $\mathbf{u}_2 \times \lambda_2 \times \mathbf{v}_2'$ ), we will get a better approximation to  $\mathbf{A}$  ( $\mathbf{A}_2$ ), but the improvement in the fit will be smaller. Adding another pair will give yet a better approximation to  $\mathbf{A}$ , but with again a smaller improvement and so on. If we were doing EOF or PCA, we would stop at the first two or three components if they explained, say, more than 50% of the structure in  $\mathbf{A}$ . In our case, however, we want to keep all  $m$  components (or most of them anyway) in order to compute the solution to the underdetermined system  $\mathbf{A}\mathbf{x} = \mathbf{b}$ .

This leaves  $n$  minus  $m$   $\mathbf{v}$  vectors that do not correspond to any  $\mathbf{u}$  vectors or  $\lambda$  scale factors. These  $n-m$  vectors represent the null space of  $\mathbf{A}$ , the part of  $\mathbf{A}$  for which we have no information. We will make use of the concept of null space later.

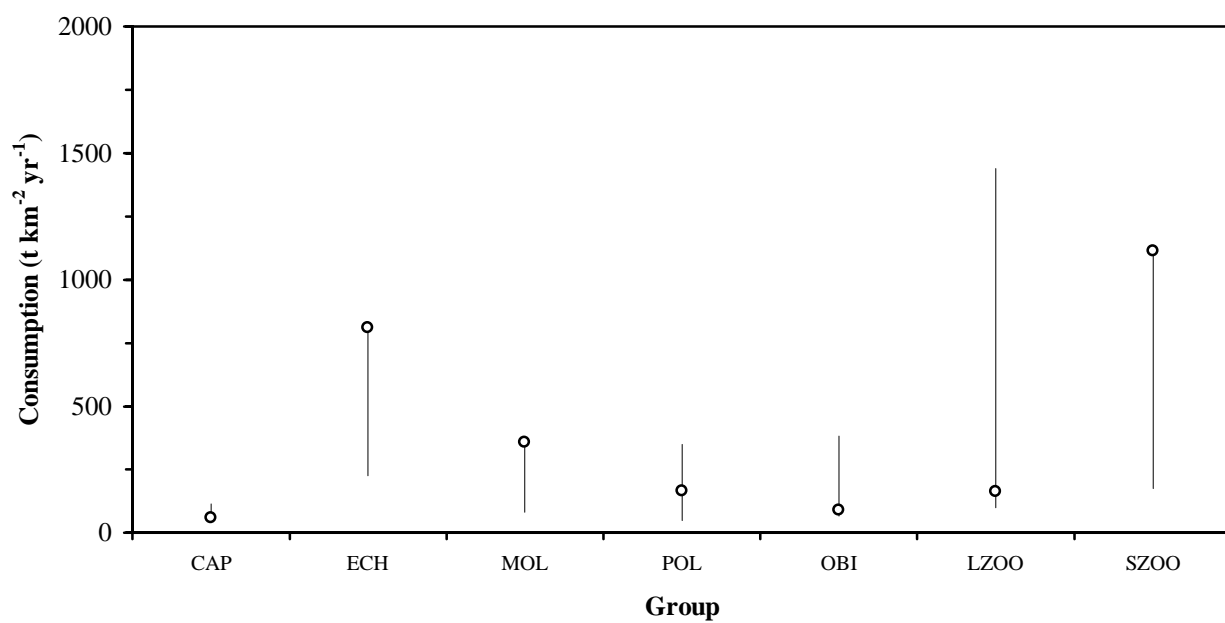
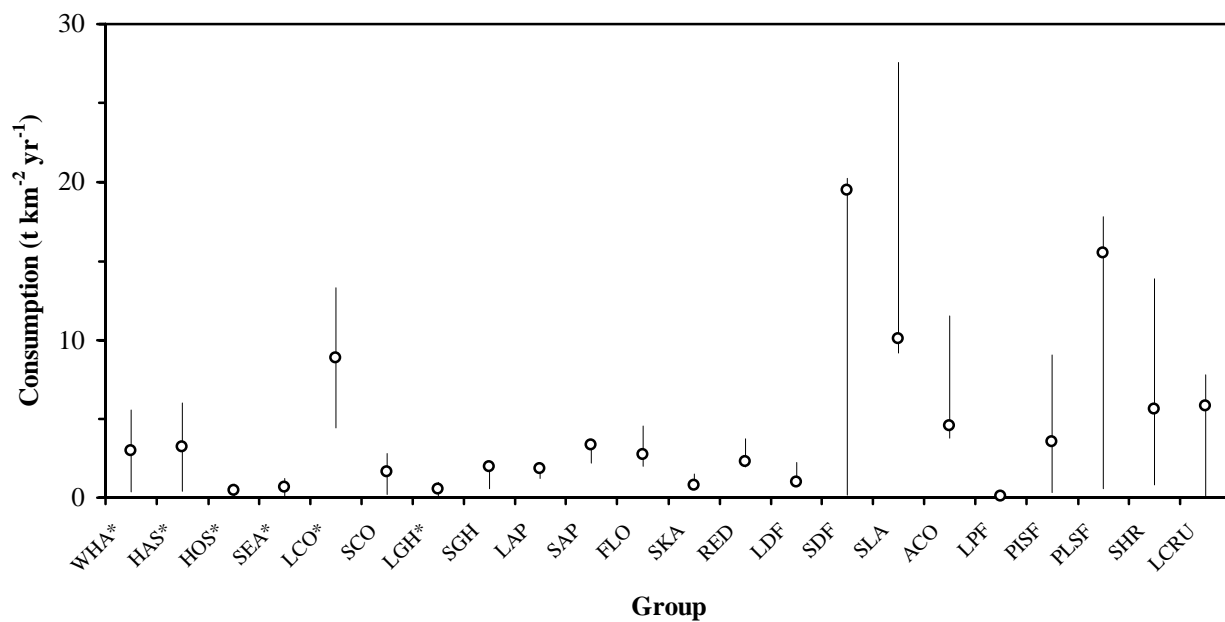
In the meantime, we can calculate a solution  $\mathbf{x}$  that satisfies  $\mathbf{A}\mathbf{x} = \mathbf{b}$  using the results from the SVD as  $\mathbf{x} = \mathbf{V} \times \mathbf{L}^{-1} \times \mathbf{U}' \times \mathbf{b}$ . The solution for our simple example (PZD) using all  $m$   $\mathbf{U}$  and  $\mathbf{V}$  vectors fits the vector  $\mathbf{b}$  exactly as expected. However, the solution contains negative flows, which are not allowed under our conceptual model.

At this point, we go back to the null space of  $\mathbf{A}$  defined above. This is  $\mathbf{V}_n$ , the  $n-m$  vectors  $\mathbf{v}_i$  that have no correspondence with the  $m$  vectors  $\mathbf{u}_i$  and scaling factors  $\lambda_i$ . This null space can be any collection of arbitrary numbers as long as they are orthogonal to each other and to the  $m$  vectors in  $\mathbf{V}$ . In addition to  $\mathbf{x}$  computed above, other solutions to the underdetermined system  $\mathbf{Ax} = \mathbf{b}$  can be constructed as  $\mathbf{x}_n = \mathbf{x} + \mathbf{V}_n \mathbf{d}$ , where  $\mathbf{d}$  is a  $(n-m \times 1)$  vector of arbitrary numbers. These other solutions fit  $\mathbf{b}$  just as well as the original solution because the  $(m-n \times n)$  null space by definition has no impact on the  $(m \times n)$  solution space. This dramatically illustrates the underdetermined nature of the problem. There is not one solution to the equations  $\mathbf{Ax} = \mathbf{b}$  but an infinity of them that we can construct at will.

Now to find the solution that respects the constraints, we need only to substitute the equation for  $\mathbf{x}_n$  into the constraint equations  $\mathbf{Gx} < \mathbf{h}$ :  $\mathbf{G}(\mathbf{x}_n + \mathbf{V}_n \mathbf{d}) < \mathbf{h}$ . Letting  $\mathbf{G}_n = \mathbf{GV}_n$  and  $\mathbf{h}_n = \mathbf{h} - \mathbf{Gx}$ , we arrive at a transformed set of inequality relations of the form  $\mathbf{G}_n \mathbf{d} < \mathbf{h}_n$ . At this point, we can use any number of algorithms to solve for  $\mathbf{d}$ , but we chose to find the smallest  $\mathbf{d}$  that satisfies these constraints. This is the quadratic programming problem of minimizing  $\|\mathbf{d}\|$  subject to  $\mathbf{G}_n \mathbf{d} < \mathbf{h}_n$ . All that has to be done is to solve this problem for  $\mathbf{d}$  and to substitute into the equation for  $\mathbf{x}_n$  above to get the new constrained solution. So, since both  $\|\mathbf{x}\|$  and  $\|\mathbf{d}\|$  are minimized,  $\|\mathbf{x}_n\|$  is also the smallest solution in the sense of minimizing the sum total of flows through the food web.

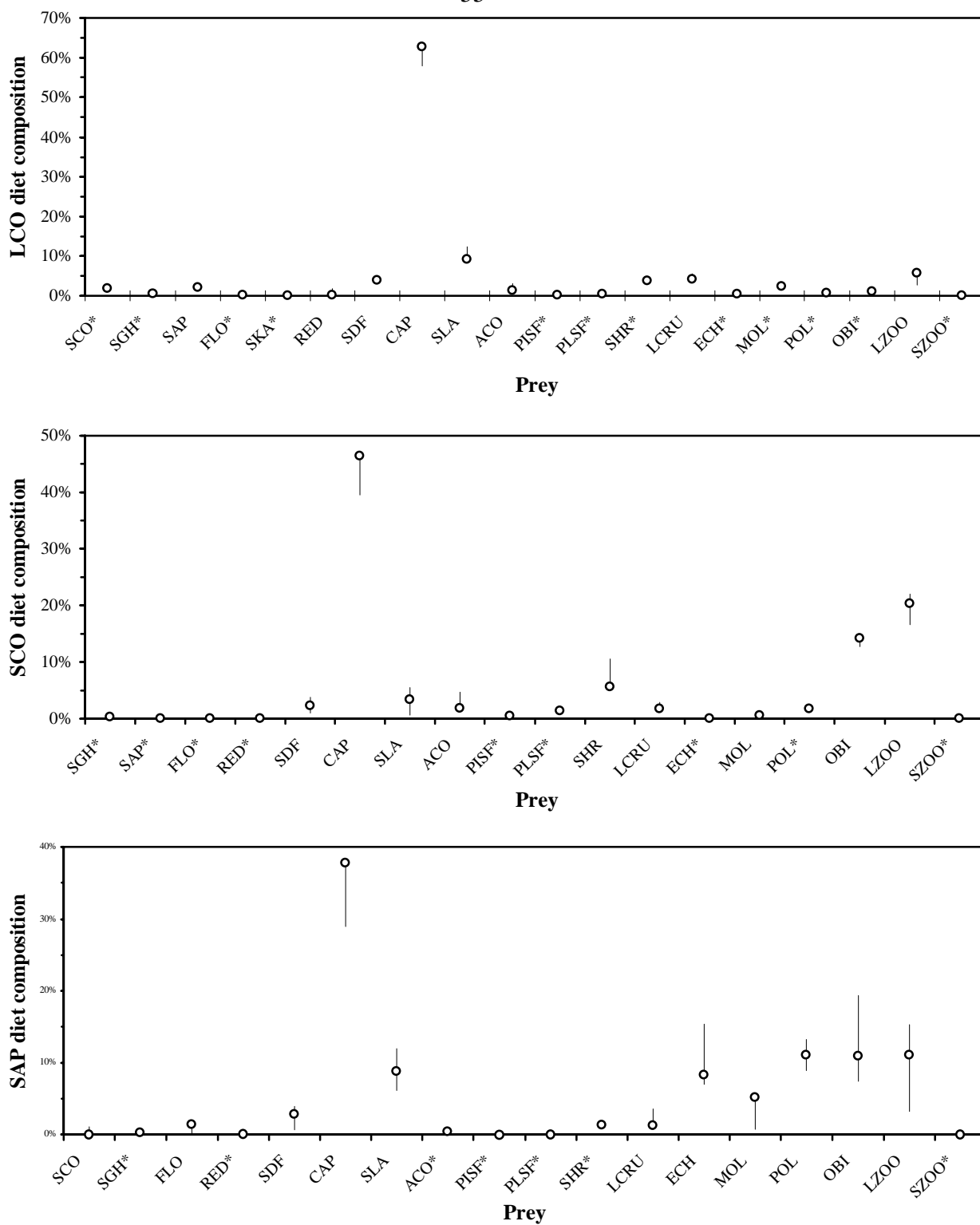
Appendix 3. Average and standard deviation of terms with large variability ( $SD > \text{mean}$ ; in  $\text{t km}^2 \text{yr}^{-1}$ ) for each inverse model. The terms near zero are in bold. A1: initial model, A2: model with modified weights for diet terms.

Large-variability terms	Model A1		Model A2	
	Average	$\pm$ SD	Average	$\pm$ SD
$\text{Pr}_{\text{LGH} \rightarrow \text{HAS}}$			$7.5 \times 10^{-3}$	$1.5 \times 10^{-2}$
$\text{Pr}_{\text{RED} \rightarrow \text{LCO}}$	$2.6 \times 10^{-2}$	$4.1 \times 10^{-2}$	$1.5 \times 10^{-2}$	$4.9 \times 10^{-2}$
$\text{Pr}_{\text{FLO} \rightarrow \text{SCO}}$	<b><math>-2.0 \times 10^{-20}</math></b>	<b><math>4.4 \times 10^{-20}</math></b>	$4.7 \times 10^{-7}$	$1.1 \times 10^{-6}$
$\text{Pr}_{\text{RED} \rightarrow \text{SCO}}$	<b><math>3.0 \times 10^{-19}</math></b>	<b><math>1.6 \times 10^{-18}</math></b>		
$\text{Pr}_{\text{MOL} \rightarrow \text{SCO}}$	$2.8 \times 10^{-3}$	$5.5 \times 10^{-3}$	$9.4 \times 10^{-3}$	$9.6 \times 10^{-3}$
$\text{Pr}_{\text{ACO} \rightarrow \text{LGH}}$	$3.9 \times 10^{-3}$	$4.4 \times 10^{-3}$	$3.9 \times 10^{-3}$	$4.4 \times 10^{-3}$
$\text{Pr}_{\text{SDF} \rightarrow \text{SGH}}$	$1.0 \times 10^{-2}$	$1.2 \times 10^{-2}$		
$\text{Pr}_{\text{SCO} \rightarrow \text{SAP}}$	<b><math>2.1 \times 10^{-14}</math></b>	<b><math>6.0 \times 10^{-14}</math></b>	<b><math>-1.8 \times 10^{-15}</math></b>	<b><math>2.6 \times 10^{-14}</math></b>
$\text{Pr}_{\text{SDF} \rightarrow \text{FLO}}$	$4.2 \times 10^{-2}$	$4.8 \times 10^{-2}$		
$\text{Pr}_{\text{SHR} \rightarrow \text{FLO}}$	<b><math>5.8 \times 10^{-15}</math></b>	<b><math>2.8 \times 10^{-14}</math></b>	<b><math>-9.5 \times 10^{-15}</math></b>	<b><math>5.2 \times 10^{-14}</math></b>
$\text{Pr}_{\text{ECH} \rightarrow \text{FLO}}$	$9.6 \times 10^{-2}$	$1.0 \times 10^{-1}$	$1.2 \times 10^{-1}$	$1.6 \times 10^{-1}$
$\text{Pr}_{\text{MOL} \rightarrow \text{FLO}}$	$8.4 \times 10^{-2}$	$9.2 \times 10^{-2}$		
$\text{M0}_{\text{RED}}$			$1.1 \times 10^{-1}$	$1.7 \times 10^{-1}$
$\text{M0}_{\text{LDF}}$	$2.5 \times 10^{-2}$	$3.0 \times 10^{-2}$		
$\text{M0}_{\text{SDF}}$			$1.5 \times 10^0$	$1.8 \times 10^0$
$\text{Pr}_{\text{SLA} \rightarrow \text{CAP}}$	<b><math>2.4 \times 10^{-14}</math></b>	<b><math>3.4 \times 10^{-13}</math></b>	<b><math>8.9 \times 10^{-14}</math></b>	<b><math>2.7 \times 10^{-13}</math></b>
$\text{M0}_{\text{SLA}}$			$5.7 \times 10^{-1}$	$6.9 \times 10^{-1}$
$\text{M0}_{\text{ACO}}$			$3.0 \times 10^{-1}$	$4.7 \times 10^{-1}$
$\text{Pr}_{\text{SHR} \rightarrow \text{LPF}}$	$8.3 \times 10^{-5}$	$2.8 \times 10^{-4}$	$7.4 \times 10^{-4}$	$1.3 \times 10^{-3}$
$\text{M0}_{\text{PLSF}}$			$7.0 \times 10^{-1}$	$1.1 \times 10^0$
$\text{Pr}_{\text{SHR} \rightarrow \text{PLSF}}$	<b><math>5.2 \times 10^{-15}</math></b>	<b><math>1.3 \times 10^{-13}</math></b>	<b><math>3.4 \times 10^{-14}</math></b>	<b><math>1.9 \times 10^{-13}</math></b>
$\text{Pr}_{\text{OBI} \rightarrow \text{PLSF}}$	<b><math>1.6 \times 10^{-14}</math></b>	<b><math>1.4 \times 10^{-13}</math></b>	$2.6 \times 10^{-1}$	$2.7 \times 10^{-1}$
$\text{M0}_{\text{LCRU}}$	$1.5 \times 10^{-1}$	$1.9 \times 10^{-1}$	$1.7 \times 10^{-1}$	$4.0 \times 10^{-1}$
$\text{Pr}_{\text{OBI} \rightarrow \text{LCRU}}$	$2.0 \times 10^{-1}$	$3.3 \times 10^{-1}$	$2.7 \times 10^{-1}$	$3.7 \times 10^{-1}$
$\text{M0}_{\text{POL}}$			$1.5 \times 10^{+1}$	$2.3 \times 10^{+1}$
$\text{M0}_{\text{OBI}}$	$8.6 \times 10^{-1}$	$2.7 \times 10^0$	$1.5 \times 10^0$	$3.2 \times 10^0$
$\text{M0}_{\text{LZOO}}$			$1.0 \times 10^{+1}$	$1.1 \times 10^{+1}$



Appendix 4. Consumption by each group estimated by the inverse A2 model. The vertical lines represent the upper and lower limits used as constraints in the inverse solution and the circles are the model estimates. An asterisk next to a group name indicates that these local measurements were used as additional equations in matrix A (no constraints).





Appendix 5. Diet composition of large cod (LCO), small cod (SCO), and small Greenland halibut (SAP) estimated by the inverse A2 model. The vertical lines represent the upper and lower limits used as constraints in the inverse solution and the circles are the model estimates. An asterisk next to a group name indicates that the diet proportion had an SD lower than 0.6% and was thus used as an additional equation in matrix A.

Appendix 6. Summary of the number of estimates that were at the limit set by the constraints for different parameters in the inverse A2 solution (sticky-constraint estimates). Q: consumption, GS: proportion of food not assimilated, GE: growth efficiency; EE: ecotrophic efficiency; Diet: diet component as a proportion of consumption. Only the estimates based on upper and lower constraint limits are shown here (there are no estimates based on additional equations). The percentage of sticky-constraint estimates obtained for the same number of estimates with the inverse A1 solution (in parentheses) are also presented for comparison.

Flow/efficiency	Number of sticky-constraint estimates	Number of total estimates	% of sticky-constraint estimates
Q	3	24	13% (38%)
GS	4	29	14% (48%)
GE	11	29	38% (59%)
EE	4	30	13% (20%)
Diet	19	94	20% (32%)
Total	41	206	20% (37%)